12-2015

# CHARACTERIZATION OF ERBB4 EXPRESSION IN OSTEOSARCOMA

Nupur Lala

# CHARACTERIZATION OF ERBB4 EXPRESSION IN OSTEOSARCOMA

By

Nupur Lala, BS

APPROVED:

Joya Chandra, Ph.D
Advisory Professor

Gary Gallick, Ph.D

Andrew Gladden, Ph.D

Winston Huh, MD

Patrick Zweidler-McKay, MD, Ph.D

APPROVED:

Dean, The University of Texas Graduate School of Biomedical Sciences at Houston

# CHARACTERIZATION OF ERBB4 EXPRESSION IN OSTEOSARCOMA

A

THESIS

Presented to the Faculty of

The University of Texas
Health Science Center at Houston
and
The University of Texas
MD Anderson Cancer Center
Graduate School of Biomedical Sciences
in Partial Fulfillment

of the Requirements

for the Degree of

MASTER OF SCIENCE

by Nupur Lala, BS
Houston, Texas

December 2015

This thesis is dedicated to my parents Meena and Parag Lala, my brother Kunal Lala and the memory of my grandmother, Mithilesh Tiwari, who would have been prouder than anyone else to see it finished.

# Acknowledgments

I would not have finished this thesis without the insight, clarity and encouragement of my advisory professor, Dr. Joya Chandra. Dr. Chandra immediately sees what is essential to solving a problem, which is the single most helpful quality I can think of in an advisor. She also has an unmatched sense of timing. Her support always arrived when it was most needed, down to her assuming the role of my advisor so that I could finish graduate school. Her advising elevated this thesis considerably. I cannot thank Dr. Chandra enough. She sets a bar that I will likely not reach. I know I will be infinitely bettered for trying, however.

Next, I owe a large debt of gratitude to my thesis committee members, Dr. Gary Gallick, Dr. Andrew Gladden, Dr. John Heymach, Dr. Winston Huh and Dr. Patrick Zweidler-McKay. I could not have asked for a better thesis committee. They helped me see the long view scientifically and professionally. I would be set if I could be a fraction as competent, enthusiastic or dedicated as they are. Their patience, humor and encouragement through this journey means more than I can convey.

I was extremely fortunate to meet Mrs. Elizabeth Escobedo Huh and Dr. Winston Huh during my time as a student. They set examples that will guide me through my professional and personal life. I cannot thank them enough. Special thanks go to Christopher, Benjamin and Madeleine Huh, who are so lovable and loving that seeing them always leaves me with lasting happiness.

A big "thank you" goes to Yanwen Yang, Tiffany Lynch and Laura Nelson of the Hughes laboratory, who helped with the data collection for my thesis. The isoform studies in this thesis would not have been completed without Yanwen's teaching and tireless assistance. Tiffany helped me assemble the *in vivo* data in this thesis. She was a boon to my scientific endeavors and I cannot wait to see where she goes in life. Laura Nelson helped me assemble and interpret the *in vivo* data. Her ideas, insights and experience were extremely valuable to shaping this thesis. I am also grateful to the members of the Hughes laboratory for their help and friendship through my time there. Special thanks goes to Kari Brewer-Savannah and Gonzalo Lopez for getting me on my feet in a wet lab.

Dr. Wei-Lien Wang of the MD Anderson Department of Pathology scored the *in vivo* data in this thesis. He was a source of help and inspiration, whether it was running back from a funeral on a Sunday afternoon to score data for my thesis committee meeting or showing me how to form hypotheses from histology. My conversations with him helped me find the questions I really wanted to ask in this thesis. Regardless of where I land in medicine, I want to be like Dr. Wang when I grow up.

Barbara Liddle kept our ship afloat in the Hughes Laboratory. Barbara was my sage and my sunshine throughout my time in graduate school and I cannot thank her enough for that. Kay Greer was also unendingly helpful and lovely. LaTausha Miles and Robin Bryce helped me so much by taking care of various loose ends and minimizing stress while I finished my thesis.

I arrived in Houston not knowing a soul and left with friends who are now family. Jasmine Dao, Callie Kwartler, Ambica Tarakad and Limin Zhu, thank you for being who you are. Bradley Lubin, thanks for being the *best* best friend through everything. I also arrived in Houston without my health. To Dr. Gary Clayman, Dr. Mohammed Habra and Dr. Bing Wang, thank you for giving my life back to me.

Thanks to my aunt and uncle Sonia and Sanjay Tiwari for all of their help, understanding and delicious food while in Houston. Finally, thank you to my parents and brother for everything in the past, present and future. I could not have asked for a better family. You all are the greatest. I will do my best to make you proud.

# Characterization of ERBB4 Expression in Osteosarcoma

Nupur Lala, BS

Advisory Professor: Joya Chandra, Ph.D

ERBB4 (Her-4) is a member of the ERBB family of Class I receptor tyrosine kinases. ERBB4 is unique within the ERBB family for alternate splicing in its juxtamembrane and cytoplasmic regions, which produces four juxtamembrane isoforms and two cytoplasmic isoforms. The cleavable juxtamembrane isoforms, Jm-a and Jm-d, can undergo proteolytic cleavage and produce an 80-kDa cytoplasmic fragment referred to as "p80," which has been demonstrated to enhance cellular survival and malignant behavior in many solid tumors [44]. ERBB4 was almost exclusively 80 kDa in size and localized to the nucleus in primary tumors and metastases in studies characterizing ERBB4 expression in osteosarcoma, indicating that ERBB4 may be cleaved to enhance malignant behavior in osteosarcoma. ERBB4 protein was significantly up-regulated from monolayer to sphere cultures in osteosarcoma, leading to the hypothesis that there would be an up-regulation of the cleavable isoforms Jm-a and Jm-d from monolayer to sphere cultures of osteosarcoma.

The first aim of this thesis was to measure if the proportion of cleavable juxtamembrane isoform expression in osteosarcoma tumor spheres from monolayer culture. All cell lines on the panel showed a significant increase in expression, by proportion or up-regulation, of at least one of the cleavable juxtamembrane isoforms Jm-a or Jm-d in sphere culture. We hypothesized that there would be a significant reduction of lung metastases with shRNA specific for Her-4 in osteosarcoma cells in xenograft mice. Immunohistochemical staining for ERBB4 was performed on sections of lungs from the experimental mice injected with CCH-OS-O cells with shRNA against ERBB4 and controls, with adjacent sections stained with vimentin as a counterstain for total osteosarcoma metastases. There were significant reductions in formation of ERBB4-

negative macrometastases (> 200 microns) in ERBB4 control mice and of ERBB4-negative micrometastases (6 cells-200 microns) in ERBB4 control and ERBB4 knockdown mice over two experiments. There was not a significant difference in the numbers of oligometastases (1-5 cells) in ERBB4 knockdown and control mice. Taken together, the immunohistochemistry suggests that ERBB4 expression may be important to metastatic progression, or formation of detectable foci, in osteosarcoma.

## *Table of Contents*

# Table of Figures

# Table of Tables



..

# Chapter 1: Introduction

## 1.1 Osteosarcoma

Osteosarcoma is a primary bone malignancy that is the third most common cancer in adolescents [1]. The majority of patients diagnosed with osteosarcoma are between the ages of 15-19 years old, with about 900 cases diagnosed per year [2]. There is a correlation between incidence of osteosarcoma and the pubertal growth spurt during which the epiphyseal growth plates of the distal femur and proximal tibia are responsible for large increases in height [3]. The most common primary sites are the distal femur, the proximal tibia and the proximal humerus [1].

Osteosarcoma is defined as a tumor of mesenchymal origin with malignant cells that produce osteoid (matrix tissue that is produced by osteoblasts, which go on to incorporate calcium and become bone) [3]. Osteosarcomas are subdivided by histological type, with conventional osteosarcoma as the most common [1]. Tumors display high histological variability, with conventional osteosarcomas forming varying amounts of fibroblastic tissue, chondroblastic tissue (cartilage) and bone [1, 3]. No significant effect has been found of predominant tumor cell type on clinical outcome [1]. Osteosarcoma is characterized by high genomic instability, with comparative genome hybridization (CGH) studies showing an average of ~9-11 chromosomal aberrations per tumor [4]. There is also a broad range of genomic instability within the disease, with studies showing some tumors with 20 or more chromosomal abnormalities and others showing none at all [5].

The most common site of osteosarcoma metastasis is the lung, with 90% of clinically detectable metastases presenting in the lungs [1]. 10-20% of patients present clinically with overt metastatic disease at time of diagnosis [1]. The outcome for patients with metastatic disease at time of initial diagnosis remains exceedingly poor, with a five-year-survival rate of

less than 30% [2]. It is estimated that 80-90% of patients have micrometastatic disease at the time of diagnosis, which is below the threshold of detection for current imaging modalities [2].

Osteosarcoma is treated with a combination of neoadjuvant chemotherapy, surgery and postoperative chemotherapy. In the pre-chemotherapy era (i.e., before 1970), the overall survival rate for osteosarcoma was less than 20% [1]. Advancements in chemotherapy protocols in the 1970's and 1980's have considerably improved survival, with a current event-free survival rate of around 70% for patients with a localized primary tumor and no evidence of overt metastatic disease at diagnosis [2]. Most chemotherapy regimens for osteosarcoma incorporate high-dose methotrexate (MDTX) with leucovorin rescue, doxorubicin (Adriamycin), cisplatin and ifosfamide [1].

Survival rates for patients with localized and metastatic osteosarcoma have plateaued since the 1980's[1, 6]. Recent insights into metastatic progression of solid tumors may improve survival rates for patients with osteosarcoma. Metastasis is the most pressing problem in the treatment of osteosarcoma, with approximately one-third of the patients initially presenting with a localized tumor developing pulmonary metastases [6]. It is estimated that 80-90% of patients with osteosarcoma have micrometastatic disease [1]. One possible route to improving survival rates is identifying progression of micrometastatic cells to clinically detectable metastases at the secondary site [6].

### 1.2 The ERBB Family of Receptor Tyrosine Kinases

ERBB4 (also referred to as Her-4) belongs to the ERBB family of Class I Receptor Tyrosine Kinases (RTK's). These RTK's are designated as Class I due to two cysteine-rich sequences in the extracellular domain [6]. The ERBB family consists of Epidermal Growth Factor Receptor (EGFR or ERBB1), ERBB2, ERBB3 and ERBB4. The ERBB family of receptor tyrosine kinases mediates signaling between the epithelium and the mesenchyme [7].

ERBB4 expression is critical to the functional and morphological late development of the fetal lung, with its deletion resulting in changes that resemble bronchopulmonary dysplasia [72]. ERBB4 is distributed in the endocrine, circulatory and nervous systems, the epithelium of the gastrointestinal, urinary, reproductive and respiratory tracts and the skin [8]. Studies of ERBB4 expression in formalin-fixed sections of adult and fetal tissues show expression levels of this receptor are higher in the developing brain and heart [8]. EGFR shows similar patterns of expression in epithelial tissues as ERBB4 along with expression in glandular epithelium, gastrointestinal tract and vascular wall smooth muscle and vascular endothelial cells [8]. ERBB2 is expressed on the epithelium of the gastrointestinal, urinary, respiratory and reproductive tracts and the skin and breast [66]. ERBB3 is expressed in the normal-term placenta, post-natal skin, lung, kidney and brain but not in skin or the fetal heart [67]. Together, this family of receptors forms the basis for a complex, layered signaling pathway that influences human growth, development and biological responses in a wide range of contexts.

The ERBB family receptors are typical receptor tyrosine kinases in structure [74]. They possess an extracellular ligand-specific binding domain, a single-pass transmembrane domain and a cytoplasmic tail with a tyrosine kinase domain [8]. The EGF-family of peptides binds to the ERBB receptors to initiate signaling [73, 74]. The EGF-family of ligands share a conserved epidermal growth factor (EGF) domain and bind with specificity to the receptors (see Figure 1.1) [7, 73].Ligand-binding to the extracellular domain of the RTK's promotes the formation of specific homodimers and heterodimers between receptors and subsequent activation of the cytoplasmic kinase domain that results in phosphorylation of specific tyrosine residues in the region [11, 73]. Dimerization may also transphosphorylation of cytoplasmic domain tyrosine residues between receptors, generating dimer-specific patterns of phosphorylation [12, 13].

EGFR and ERBB4 are autonomous [74]. They bind EGF-like ligand, dimerize and generate downstream signaling that affect growth and proliferation [73-74]. An important characteristic of the ERBB family is that ERBB2 and ERBB3 are non-autonomous [74]. ERBB2 is unable to bind EGF-like ligands but is activated by heterodimerization with ligand-bound receptors [73-74]. ERBB2 acts as the preferred heterodimerization partner for the other three members of the ERBB family [7, 74]. ERBB3 lacks constitutive kinase activity and only undergoes tyrosine phosphorylation through heterodimerization with other receptors [7, 74].

ERBB4 is unique with the ERBB family for alternate transcriptional splicing that produces four juxtamembrane isoforms and two cytoplasmic isoforms. The juxtamembrane isoforms Jm-a and Jm-d contain a 23-amino acid sequence that confer susceptibility to proteolytic cleavage, creating an 80-kDa fragment that may translocate to the nucleus to affect downstream signaling. The cytoplasmic isoforms Cyt1 and Cyt2 isoforms differ in their recruitment of PI3K, with Cyt1 containing a binding site for PI3K. Binding of ligands such as EGF to EGFR or the Neuregulins to ERBB4 stimulates ERBB4 homodimerization [7]. ERBB4 forms homodimers upon binding of the Neuregulins and forms heterodimers with the EGFR receptor and ERBB2 receptors [7].

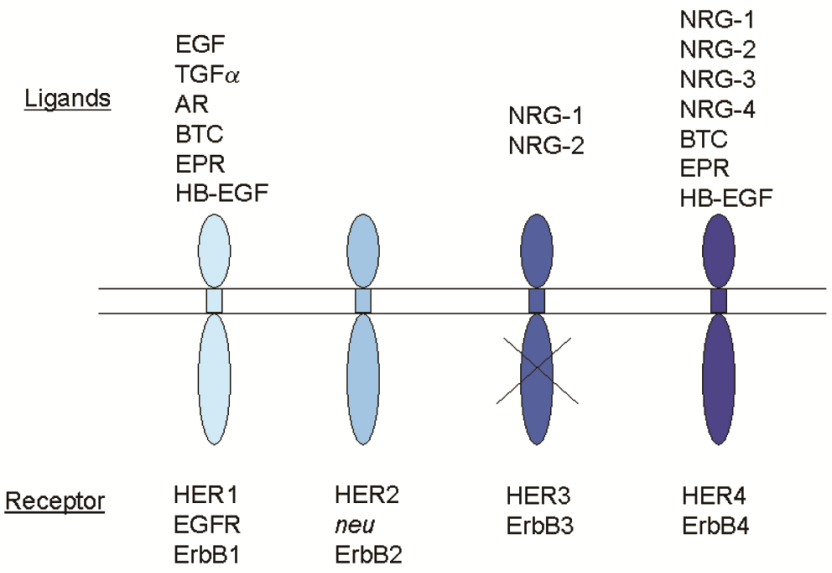


**Figure 1.1: The RTK's of the ERBB family with their associated extracellular ligands.** All members of the ERBB family contain an extracellular ligand-binding domain, a single-pass transmembrane domain and an intracellular domain with tyrosine kinase activity [12]. The extracellular domain conformation of ERBB2 makes it unable to bind ligand but enables dimerization in spite of this, making it the preferred heterodimerization partner of the other ERBB family members. The ERBB3 receptor lacks constitutive kinase activity. Figure taken from Lin and Winer, *Breast Cancer Res* 2004 **6**: 204-210

The phosphotyrosines recruit proteins with phosphotyrosine binding (PTB) domains, adaptor proteins or effector proteins with Src homology (SH2) binding domains, activating a variety of downstream signaling pathways [10]. ERBB4 recruits GRB2, Shc and STAT5 [73-74].

When a ligand (EGF-like or neuregulin) binds to EGFR, ERBB3 or ERBB4, homodimerization is induced. Homodimers of EGFR and ERBB4 signal weakly in comparison to ERBB2-containing heterodimers, which are the most mitogenic of the ERBB dimers [7, 12]. A consensus has been reached through studies in breast cancer models that the ERBB2-ERBB3 heterodimer is the ERBB heterodimer with the most mitogenic signaling potential.

The possible combinatorial interactions between ligands, receptors, dimers and signaling proteins within the ERBB family form the basis for a highly diverse and interactive network. Signaling proteins that bind to the phosphorylated tyrosine residues on the kinase domain confer control of the duration and strength of downstream signaling in a variety of developmental processes [10]. Ligands and dimerization partners, as well as the distinct phosphorylation

pattern on the cytoplasmic tails of individual receptor, determine the pattern of tyrosine phosphorylation to activate downstream signaling pathways [15].

### 1.3 Signaling Pathways Coupled to the ERBB Family

Ras-MAPK, PLC-PKC and PI3-Kinase/Akt are the three primary signaling pathways coupled to ERBB signaling that have been most extensively studied [10]. The Ras-MAPK pathway is activated by all of the ERBB ligands and receptors. Ras-MAPK serves to regulate cell proliferation, survival, growth and migration [16]. All RTK's stimulate exchange of GTP for GDP on the G protein Ras [13]. Ras is activated by the guanine nucleotide exchange factor Sos [13]. One pathway of Ras-MAPK activation by ERBB family members occurs through binding of the SH2-domain on the adaptor protein Grb-2 to the PTB domain of the ERBB receptors [10, 13]. Sos binds with the SH3 domains of Grb-2 to form a Sos/Grb-2 complex [13]. The binding of the SH2 domain of Grb-2 to specific phosphotyrosines on the receptor enables the translocation of Sos close to Ras at the plasma membrane, where Sos promotes exchange of GTP for GDP to activate Ras [13]. The Sos/Grb-2 complex may also position Sos close to Ras on the plasma membrane through binding to Shc, an adaptor protein that binds to several receptors through its PTB domain [10, 13].

Phospholipase Cγ (PLCγ) binds to phosphotyrosines on activated EGRF and ERBB2 via its SH2 domains [10]. PLCγ is activated by phosphorylation by RTK's [10]. Activation of PLCγ results in PLCγ hydrolyzing its substrate to form two second messengers, diacylglycerol (DAG) and inositol triphosphate ($IP_3$) [10, 13]. $IP_3$ binds to intracellular receptors to stimulate intracellular calcium ($Ca^{2+}$) release [10, 13] . $Ca^{2+}$ subsequently binds to calmodulin to activate $Ca^{2+}$/calmodulin-dependent protein kinases [13]. DAG and $Ca^{2+}$ activate Protein Kinase C (PKC), which phosphorylates a variety of substrates to trigger diverse signaling events [13, 17].

PI3K is activated by all of the ERBB receptors. The PI3K family that directly interacts with the ERBB receptors consists of heterodimers containing two SH2 domains, one SH3 domain, a regulatory p85 subunit and a catalytic p110 subunit [13]. PI3K activation is coupled to ERBB receptors via GTP-Ras binding to the p110 subunit of PI3K [10]. There is also SH2-mediated recruitment by the activated ERBB receptors of the p85 regulatory subunit of PI3K [10]. The degree of PI3K activation is receptor-dependent. ERBB3, upon heterodimerization, can recruit PI3K to six distinct putative p85 binding sites on its cytoplasmic domain [10]. ERBB4 contains one putative p85 binding site whereas adaptor proteins mediate the interaction between PI3K and the EGFR and ERBB2 receptors, resulting in weaker PI3K activation by the EGFR and ERBB2 receptors [10]. PI3K signaling promotes proliferation and enhanced survival [10].

ERBB signaling is attenuated primarily through ligand-mediated receptor endocytosis. There is high turnover of the receptors at the plasma membrane due to both ligand-induced and ligand-independent endocytosis. Exposure to the EGF ligand hastens the internalization rate of the EGFR receptor by ten-fold due to phosphorylation of the clathrin adaptor protein Eps15 [9]. EGF- ligand mediated coupling of the E3 ubiquitin ligase Cbl to EGFR-homodimers results in ubiquitination of the receptors, which marks them for endocytosis and lysosomal degradation [9, 12]. ERBB2 and ERBB3 do not undergo ligand-mediated proteolysis and are instead recycled to the membrane where they undergo repeat activation by ligand binding [12].

### 1.4 Biology of the ERBB4 Receptor Tyrosine Kinase

ERBB4 is an emerging target due to recent insights into its complex biology and effects on tumorigenesis .The ERBB family has been an active target of investigation within cancer biology since the early 1980's [20]. Dysregulation of ERBB signaling at the input (ligand and receptor) and output (downstream signaling) layers have been implicated in the development

and maintenance of several solid tumors [7, 20]. EGFR, ERBB2 and ERBB3 have been extensively studied in the context of solid tumors.

ERBB4 is a 180-kDa protein with structure homologous to the other ERBB family members. ERBB4 is expressed in multiple mammalian tissues, including the cerebral cortex, the intestinal tract and developing cardiac myocytes. Ligand binding stimulates homodimerization and heterodimerization with EGFR, ERBB2 and ERBB3, kinase activation and phosphorylation of tyrosine residues on the kinase and carboxyl domain.

ERBB4 is unique within the ERBB family for its functionally distinct alternate juxtamembrane and cytoplasmic isoforms generated by alternate splicing. The Jm-a and Jm-d isoforms contain an alternate 23-amino acid sequence encoded by exon 16 (see Figure 1.2) in the juxtamembrane region, which confers sensitivity to a two-step proteolytic cleavage process after ligand-binding. First, the receptor is cleaved by TACE (tumor necrosis factor-α converting enzyme). The extracellular domain of the receptor is shedded, leaving an 80-kDa cytoplasmic fragment attached to the membrane [21]. In a consecutive second step, presenilin-dependent γ-secretase cleaves the cytoplasmic fragment from the membrane to create a soluble 80-kDa cytoplasmic ("p80") fragment that is capable of translocating to the nucleus and behaving as a transcription factor [21, 22].

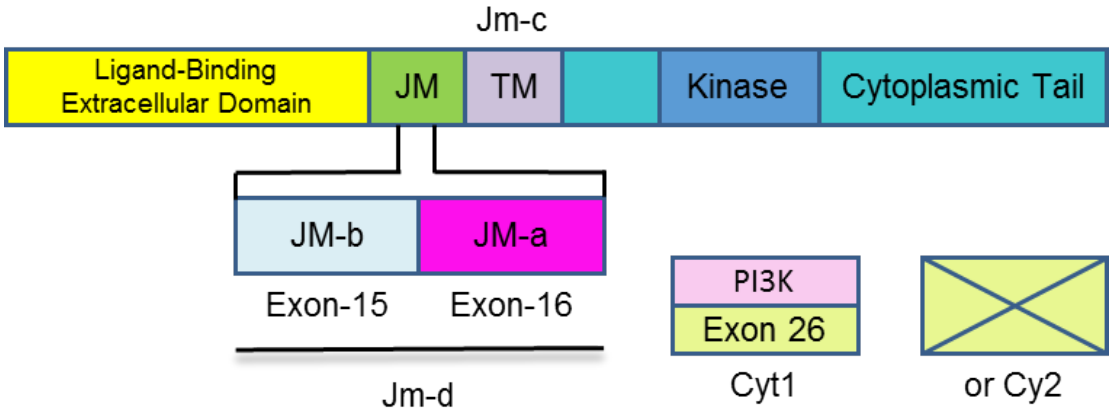


**Figure 1.2: The juxtamembrane and cytoplasmic splice isoforms of ERBB4.** ERBB4 contains an extracellular domain that binds ligand. Alternate splicing in the juxtamembrane (JM) region produces the cleavable Jm-a (Exon 16) or non-cleavable Jm-b (Exon 15) isoform. The JM region is deleted in the Jm-c isoform. Jm-d contains both exons and is susceptible to cleavage. The cytoplasmic tail contains a kinase domain that is activated after ligand binding. Splicing in the cytoplasmic region produces the Cyt1-isoform with a PI3K binding site in exon 26 or the Cyt2-isoform with deletion of exon 26 and loss of the PI3K binding site.

The Jm-b isoform contains an alternate 13-amino acid sequence encoded by Exon 15 and lacks the amino acid sequence encoded by Exon 16 that confers susceptibility to proteolytic cleavage. The Jm-c and Jm-d isoforms were first reported in medulloblastoma [23]. The Jm-d isoform contains both of the sequences Exon 15 and 16 and the Jm-c isoform contains a deletion of the entire juxtamembrane region [23, 24]. Thus, Jm-c is a non-cleavable isoform of ERBB4 and Jm-d is a cleavable isoform of ERBB4.

The p80 fragment of ERBB4 exerts influences on a broad range of cellular signaling and behavior (see Figure 1.3) [25]. Two alternate cytoplasmic fragments are created from the cytoplasmic isoforms of ERBB4. ERBB4 cytoplasmic isoforms are generated from the inclusion (Cyt-1) or deletion (Cyt-2) of a 16-amino acid sequence, which enables the direct interaction of PI3K/Akt with the Cyt-1 isoform [26]. The p80 fragment may remain in the cytoplasm or translocate to the nucleus to regulate gene expression [27]. The p80 fragment may also

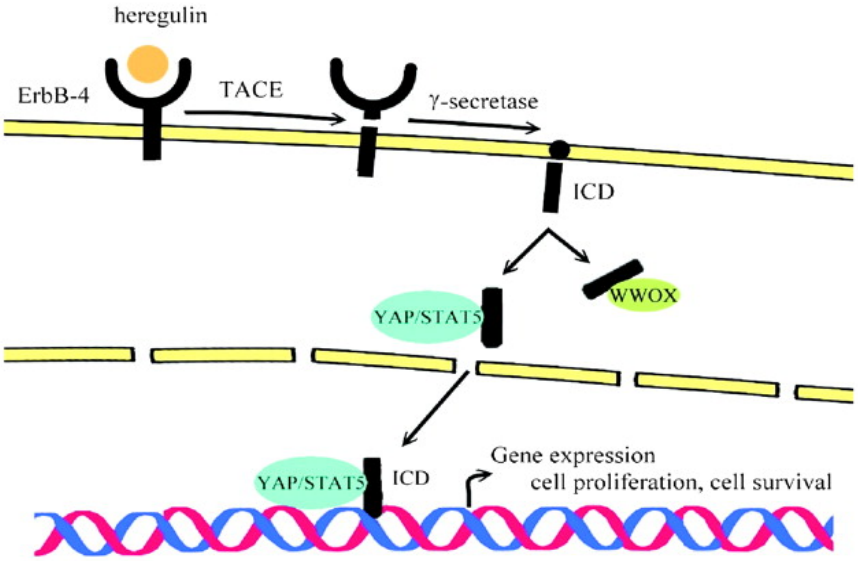


**Figure 1.3: Signaling of the ERBB4 p80 fragment (ICD).** Binding of ligand stimulates two-step proteolytic cleavage by TACE and γ-secretase of ERBB4 isoforms containing a 23-amino acid recognition sequence that renders susceptibility to proteolytic cleavage. This creates an 80-kDa fragment of the ERBB4 ICD, also known as "p80," which exerts effects downstream effects on signaling. The ICD fragment may translocate to the nucleus, where it may activate signaling by YAP, STAT5 or WWOX. Chuu, C.P., Chen, R.Y., Barkinge, J.L., Ciaccio, M.F. and R.B. Jones. Molecular Cancer Research, 2008, **6**(6), pp. 885-891.

accumulate in the mitochondria and activate BAK through its BH3-like domain, resulting in membrane permeabilization and cytochrome efflux which commits cells to the intrinsic apoptotic pathway [28]. The fragment affects gene transcription through its interaction with downstream transcriptional co-activators such as YAP, WWOX and Stat5 [29, 30]. Both YAP and WWOX interact with the p80 fragment through their Group 1 WW-domains, sequences of 35-40 amino acids that bind proline-rich motifs on proteins [27, 31]. Group 1 WW-domains bind to PPxY consensus motifs, in which P represents Proline, x is for any amino acid and Y is for tyrosine [27]. The Cyt-1 isoform of ERBB4 contains three PPxY motifs; the Cyt-2 isoform contains two PPxY motifs. The WW-domains on YAP associate with the PPxY motifs in the cytoplasmic fragment of ERBB4 to translocate the p80 fragment to the nucleus and co-activate its transcriptional function [27]. The p80 fragment generated through proteolytic cleavage regulates transcription of several currently unidentified genes involved in a variety of cellular

processes, including embryonic differentiation [27, 32]. PKC stimulates cleavage of ERBB4, creating an 80-kDa cytoplasmic fragment that lacks independent kinase activity but that contains phosphotyrosines that interact with the SH-2 domain of PLCγ [18].

WWOX functions as a tumor suppressor gene in neuroblastoma, Wilms' tumor and breast cancer [29, 33, 34]. WWOX competes with YAP for binding to PPxY motifs on the p80 fragment in the cytoplasm [27]. WWOX opposes the actions of YAP by segregating the p80 fragment in the cytoplasm and halting its transcriptional activity [27].

ERBB4 activates Signal transducer and activator of transcription (STAT) family member STAT5A in mammary tissue [35]. The p80 fragment functions as a nuclear chaperone for STAT5, trans-activating genes that are responsible for mammary differentiation and milk production during lactation [35]. STAT5A also mediates accumulation of the p80 fragment within the nucleus but the biological consequences of this are yet to be established [35]. Activation of STAT5 is linked to transformation in several cancers [25].

### 1.5 ERBB4 Signaling in Osteosarcoma

Previous data on the expression patterns of the ERBB family members in osteosarcoma showed that ERBB4 protein was detected primarily as a fragment of $M_f$ 80,000 in Western blots of primary osteosarcoma cell lines WOL and Saos2 [75]. Immunohistochemical staining for ERBB4 expression performed on paraffin-embedded blocks made from WOL, Saos2 and primary osteosarcoma line SJSA supported this observation, with ERBB4-antigen displaying nuclear localization [75]. Immunohistochemistry to assess ERBB4 expression in archival tumor samples showed near-complete nuclear localization [75]. 2-D gel electrophoresis employed on WOL treated with an ERBB-phosphorylation inhibitor showed that dephosphorylation of WOL was consistent with dephosphorylation of the p80 fragment of ERBB4 [76]. These observations

collectively suggest that ERBB4 signaling in primary osteosarcoma cell lines may be mediated through the p80 fragment created with proteolytic cleavage by TACE and γ-secretase [76].

The role of ERBB4 in cancer progression or suppression is controversial. ERBB4 expression increases metastatic potential in solid tumors including breast cancer, lung cancer, thyroid cancer and melanoma [36-39]. ERBB4 expression has been linked to enhanced proliferation in lung cancer cells and breast cancer cells [37, 38]. Mutated ERBB4 receptors in melanoma activate dysregulated ERBB4 and PI3K-Akt signaling [40]. Knockdown of ERBB4 mutants blocked proliferation of melanoma cells while growth remained unaffected by knockdown of wild-type ERBB4, which indicates that specific mutations must be present on ERBB4 to promote oncogenic growth and signaling in melanoma [41]. ERBB4 may function as an oncogene in thyroid cancer due to its strong expression in thyroid cancer cell lines in which migration, chemotaxis and metastasis is stimulated by the ERBB4 ligand HB-EGF (heparin-binding EGF-like growth factor) [36]. Alternately, ERBB4 is implicated as having tumor-suppressive function in estrogen receptor-positive breast cancers due to its association with elevated levels of estrogen receptor expression [42]. Recent studies have demonstrated that a functional kinase domain must be present on the expressed receptors for ERBB4 to inhibit proliferation in breast cancer, prostate cancer and pancreatic cancer cell lines [43].

The splicing of a single ERBB4 gene to create four juxtamembrane isoforms with varying expression patterns and differing function underlies the difficulty in identifying the role of ERBB4 in cancer progression or suppression. All ERBB4-expressing tissues, normal or malignant, express both Cyt-1 and Cyt-2 cytoplasmic isoforms in varying proportions [44]. Not all juxtamembrane isoforms are expressed in all ERBB4-expressing tissues, however. There is an increase in expression of cleavable juxtamembrane isoform mRNA transcripts of ERBB4 across cancers [44]. Breast cancers and melanoma seem to exclusively express the Jm-a isoform

while cancers such as ovarian cancer and medulloblastoma that express the less frequently-observed Jm-c and Jm-d isoforms show an increase in the proportion of cleavable (Jm-a and Jm-d) to non-cleavable isoforms (Jm-b and Jm-c) [23, 41, 45].

Cleavable juxtamembrane isoform expression of ERBB4 is linked to worse prognosis in solid tumors. Increased nuclear localization of the p80 fragment in breast cancer cells was associated with decreased survival in breast cancer patients [45]. Elevated levels of the ERBB4 ectodomain were measured in the serum of breast cancer patients as compared to no expression of the ERBB4 ectodomain in healthy controls [46]. Blocking cleavage of ERBB4 with an anti-ERBB4 antibody that bound to the region containing the residues recognized for proteolytic cleavage diminished cleavage both *in vitro* and *in vivo* and suppression of growth in breast cancer xenografts in mice [46]. Expression of the cleavable Jm-a and Jm-d isoforms in medulloblastoma and pilocytic astrocytoma was elevated in comparison to expression in normal brain tissue while transcripts of TACE and γ-secretase were similar across medulloblastoma, pilocytic astrocytoma and normal tissue samples. Taken together, this data suggests that increased proteolytic cleavage of ERBB4 may be more prevalent in those tumor types and may contribute to aberrant signaling from normal brain tissue [24].

Specific expression of juxtamembrane isoforms of ERBB4 drives the receptor's effects on cell growth, survival and apoptosis [44, 47-49]. Fibroblasts transfected with the Jm-a Cyt-2 receptor showed enhanced proliferation, anchorage-independent survival and resistance to serum starvation compared to fibroblasts transfected with the Jm-b Cyt-2 receptor [48]. Overexpression of the Jm-a Cyt-2 isoform in interleukin-3-independent myeloid 32D cells resulted in ligand-independent proliferation, which was not observed with Jm-a Cyt-1 or either of the Jm-b cytoplasmic isoforms [30]. Fibroblasts expressing the Jm-b receptor showed an increase in cell death in serum-free conditions over both fibroblasts expressing the Jm-a receptor

and control cells, indicating that the Jm-b receptor may confer sensitivity to apoptosis in conditions of nutrient deficiency [48]. Treatment of MCF-7 breast cancer cells with an anti-ERBB4 antibody that selectively binds to the Jm-a isoform significantly reduced their proliferation and anchorage-independent growth [50].

### 1.6 ERBB4 Is Up-Regulated in Anchorage-Independent Culture

ERBB4 enhances tolerance to pro-apoptotic cellular stressors in neuroblastoma and Ewing's sarcoma [51, 52]. Neuroblastoma cell lines showed up-regulation of total ERBB4 protein in anchorage-independent cell culture compared to monolayer cell culture [52]. Anchorage-independent growth may be used as a proxy for cells' ability to survive and proliferate without attachment to extracellular matrix [53]. ERBB4 may be the member of the ERBB family that mediates multicellular resistance in neuroblastoma cell lines, as there was no up-regulation measured of the other ERBB family members from monolayer to anchorage-independent cultures [52]. Knockdown of ERBB4 in neuroblastoma cells increased neuroblastoma cells' chemosensitivity while lowering their anchorage-independent survival and tolerance to serum starvation [52].

Cells from neuroblastoma and Ewing's sarcoma cell lines aggregate with each other to form tumor "spheroids" in anchorage-independent culture conditions [52, 53]. Tumor spheroids are three-dimensional aggregates of viable cancer cells that form in culture upon inhibition of attachment to tissue culture plastic. Gene expression profiles of tumor spheroids been found to display greater overlap with those of clinical tumor samples in models of colon and epithelial ovarian cancers and hepatocellular carcinoma [54]. Spheroids more closely resemble solid tumors *in vivo* due to stronger cell-cell adhesion than cells grown in monolayer culture, hypoxic centers and a mixture of viable and necrotic cells within each spheroid [52]. The increased cell-

cell contact found in tumor spheroids is thought to contribute to their enhanced chemoresistance [52, 54].

### 1.7 Rationale for Thesis

Knockdown of ERBB4 resulted in a higher percentage of neuroblastoma cells grown in tumor spheroids undergoing apoptosis than single cells grown in monolayer culture [52]. These findings, in combination with observed up-regulation of ERBB4 in tumor spheroids of neuroblastoma from monolayer culture, suggest that ERBB4 may be important to cell survival in conditions of loss of attachment to matrix [52].

ERBB4 resists characterization as an oncogene or a tumor suppressor because its role is partially determined by the functionally different isoforms expressed within the tumor. Overexpression of the cleavable juxtamembrane isoform Jm-a Cyt-2 significantly enhanced anchorage-independent survival in both normal fibroblasts and breast cancer cells while overexpression of the non-cleavable Jm-b Cyt-2 isoform increased apoptosis of both cell types in anchorage-independent conditions [48]. Immunohistochemical staining of ERBB4 in clinical samples from estrogen receptor (ER)-positive breast cancers showed that strong ERBB4 staining was linked with favorable outcomes in patients but increased nuclear expression of the cleaved p80 fragment of ERBB4 in the tumor tissue was associated with poorer clinical outcomes [58]. The localization of ERBB4, driven by the cleavable juxtamembrane isoform expression, underlies effects of ERBB4 on breast cancer progression [58].

Previous data from our laboratory showed an up-regulation in total ERBB4 protein from monolayer to anchorage-independent culture in three osteosarcoma lines, CCH-OS-O, CCH-OS-D and Saos2 (see Fig.1.4). These three cell lines formed tumor spheroids in anchorage-independent culture [52]. In studies with neuroblastoma cells, ERBB4 expression was up-regulated in neuroblastoma spheroids [52]. The up-regulation in ERBB4 was associated with the

neuroblastoma spheroids increasing multicellular resistance (MCR), which is intrinsic resistance to adverse conditions that occurs from tumor cells' three-dimensional configurations [52].

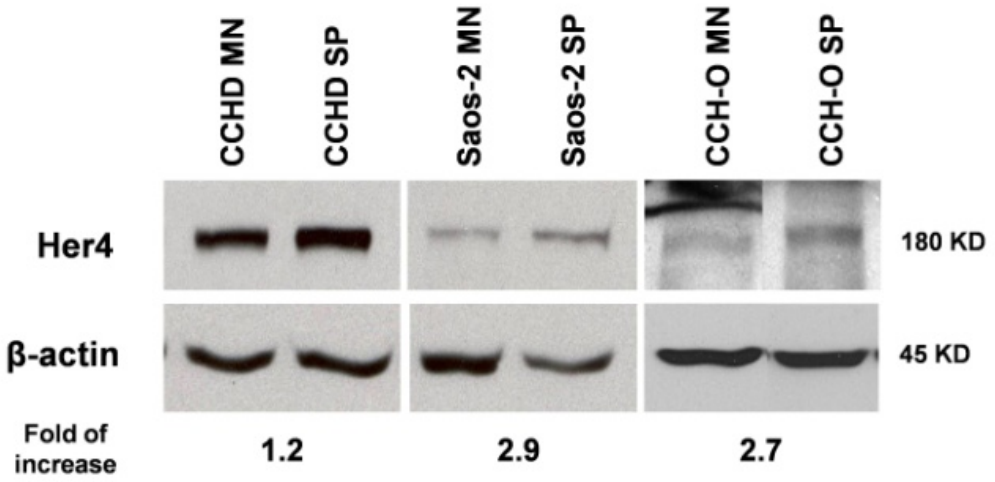


**Figure 1.4: Total ERBB4 protein is upregulated in tumor spheroids.** Osteosarcoma cell lines CCH-OS-O, CCH-OS-D and Saos2 were grown in monolayer culture and anchorage-independent culture. The cells spontaneously formed tumor spheroids. The cell lines show up-regulation of total ERBB4 protein from monolayer (MN) to spheroid (SP) culture, suggesting that tumor spheroids up-regulate ERBB4 in response to survive in anchorage-independent conditions. Western blot and densitometry analysis performed by Dr. Yingqi Hua, MD, Hughes Laboratory.

Osteosarcoma cells aggregated to form tumor spheroids and up-regulated ERBB4 in response to anchorage-independent conditions, as also observed in neuroblastoma and Ewing's. In neuroblastoma, total ERBB4 protein expression increased as culture confluence increased [52]. ERBB4 may be up-regulated in conditions of higher confluence because of cell-cell contact itself or stress induced by increased contact [52]. To test if increased cell-cell contact affected juxtamembrane isoform expression, we included a "high density" culture condition in which osteosarcoma cells were grown to complete confluence in monolayer culture. The "high density" condition was an intermediate between sub-confluent conventional monolayer culture and the stronger cell-cell contact and increased interactions between cells in tumor spheroids [54].

Overexpression of cleavable ERBB4 juxtamembrane isoforms significantly increased anchorage-independent survival in normal and tumor tissues [37, 48]. Taken with previous studies demonstrating that ERBB4 expression was largely nuclear in primary osteosarcoma cell lines, we wished to determine if the expression of cleavable isoforms of ERBB4was altered from monolayer to tumor sphere cultures of primary osteosarcoma lines. The second set of experiments that form the basis for this thesis are immunohistochemical analyses on the lungs and tibias of mice injected with osteosarcoma cells with ERBB4 knockdown. Our aims were to determine if ERBB4 expression increased in osteosarcoma metastases than primary tumors because of its up-regulation in a condition in which cell-cell contact was integral to survival and if knockdown of ERBB4 affected metastasis formation. Together, we wanted these experiments to elucidate a role of ERBB4 in the progression of micrometastases to macrometastases in osteosarcoma. **We hypothesized that there would be an increased proportion of cleavable ERBB4 juxtamembrane isoform expression in anchorage-independent multi-cellular tumor spheroids and as a result, ERBB4 knockdown would result in a reduction in size and number of osteosarcoma metastases.**

# Chapter 2: Materials and Methods

## 2.1 Cell Culture and Experimental Reagents

Human osteosarcoma cell lines CCH-OS-D, Saos2, CCH-OS-O and CCH-OS-K were selected for their up-regulation of ERBB4 protein in tumor spheroids, as detected by previous Western blots in the Hughes Laboratory (see Figure 1.4). Cell lines CCH-OS-D, CCH-OS-O and CCH-OS-K were generated from primary tumor samples obtained from patient biopsies perform at the Children's Cancer Hospital at MD Anderson Cancer Center. Saos2 is an established osteosarcoma line from the ATCC Cell Biology Collection, a non-profit organization dedicated to the collection and maintenance of established cell lines for experimental purposes.

CCH-OS-D, Saos2, CCH-OS-O and CCH-OS-K were grown in Dulbecco's Modified Eagle Medium (DMEM)/1X Media (Life Technologies, Carlsbad, CA) or DMEM/High Glucose Media (HyClone, Logan, UT). Both media contained 4500 mg/L Glucose, L-Glutamine and Sodium Pyruvate. All media was supplemented with 10% Fetal Bovine Serum (FBS) (HyClone, Logan, UT) and 1% Penicillin/Streptomycin Amphotericin B (Lonza Inc., sites worldwide).

Cells were maintained in three culture conditions for RNA extraction: monolayer (MN), high density (HD) and anchorage-independent, or "sphere" culture (SP). All cells were incubated at 37º Celsius with 5% $CO_2$. Both the monolayer and high density cultures were adherent cultures plated in 10-cm dishes. CCH-OS-D was plated at 10^5/mL due to its relatively short doubling time of 12-14 hours and its enhanced growth observed with cell-cell contact. CCH-OS-O and CCH-OS-K were plated at $3x10^5$/mL. Saos2 was plated at $5x10^5$/mL because its growth in culture was arrested without cell-cell contact. The monolayer cultures were grown until cells had reached sub-confluence. Monolayer cultures of CCH-OS-D, CCH-OS-O and CCH-OS-K were collected before cells made contact on the plate at 60-70% confluency. Saos2

would be collected at 70-80% confluency in monolayer culture due to its larger cell size and growth only in conditions of cell-cell contact.

Cells in high-density cultures were allowed to grow until growth either halted due to contact inhibition or until cells looked healthy and viable by visual inspection under a microscope. Saos2 experienced contact inhibition so its cultures were harvested at 90% confluency. CCH-OS-D, CCH-OS-O and CCH-OS-K did not display any contact inhibition, growing in layers upon each other when there was no available surface on the plate. These cell lines were harvested at confluency. They were monitored under the microscope regularly to ensure that harvesting occurred before cells started to display necrosis

Cells grown in anchorage-independent culture conditions were plated at $10^{6/}$well in six-well plates with the culture surfaces coated in Poly-Hema, a polymer used in cell culture to inhibit cell adhesion. Each well was coated with 2 mL of 5% Poly-Hema (Poly(2-hydroxyethyl methacrylate) solution per well (Sigma-Aldrich, St. Louis, MO). The Poly-Hema solution was prepared according to the manufacturer instructions prior to use. The six-well plates were coated with Poly-Hema solution and left to dry completely (12-14 hours) in a sterilized cell culture hood prior to use.

Cells from all cell lines spontaneously formed tumor spheroids or “spheres,” sphere-shaped aggregates of cells that survive anchorage-independent conditions. The spheres were incubated for 4 days at a time so that incubation times were identical to those of theWestern blots that showed up-regulation of ERBB4 in sphere cultures of those cell lines (see Figure 1.4). . RNA was isolated from cells post-incubation.

## 2.2 Preparation of RNA and cDNA

### *2.2a Preparation of Monolayer and High Density Cultures for RNA Extraction*

All media was removed with pipetting from monolayer and high density cultures. Cells were washed with 3 mL of Hanks' 1X Balanced Salt Solution (Life Technologies, Carlsbad, CA). Next cells were incubated in the cell incubator with 1.5 mL of cold TrypLE Express Recombinant Enzyme with EDTA, a direct replacement for trypsin (Life Technologies, Carlsbad, CA). Cells were incubated with trypsin until they detached from the plate, which took from five minutes to ten minutes for the most highly adherent cultures. Once cells had detached from the plate, 3 mL of fresh media was added to the culture plate to halt the reaction with trypsin (2:1 ratio of media:trypsin is necessary to halt enzymatic reaction). 0.5 mL of the cell suspension was collected from each plate for counting in the Vi-Cell Cell Viability Analyzer XR.204 (Beckman Coulter, Fullerton, CA). This instrument was used to quantify the number of viable cells per milliliter of suspension, which was used to calculate the volume of suspension necessary for RNA extraction. The remaining media/trypsin suspension from each plate was collected in a clean 15-mL centrifugation tube and centrifuged at 1300 rpm for 4 minutes at 4ºC.

After a cell count was obtained, the formula $2x10^6$/(number of viable cells/mL) was used to find the volume of cell suspension from each tube that was needed to create a pellet with approximately $2x10^6$ cells. The media from the previous centrifugation was removed and the cells were re-suspended in fresh media. The correct volume of cell suspension to create a pellet of approximately $2x10^6$ cells was pipetted into a fresh 15-mL centrifugation tube and spun down again in the centrifuge at 1300 rpm for 4 minutes at 4º C. The media was removed from the pellet and the pellet was resuspended in 1.0 mL of 1X HBSS. This procedure was employed to clean the remaining media from the cells prior to RNA extraction. The pellet-HBSS suspension was transferred to a clean 1.5 mL Eppendorf tube (Sigma-Aldrich, St. Louis, MO) in which it

would be spun at 8.0 G for 5 minutes in an accuSpin Micro 17 Microcentrifuge (Fisher Scientific, Waltham, MA). At the end of this centrifugation would be left a clean pellet of roughly $2x10^6$ cells that was ready for extraction of RNA.

***2.2b Preparation of Sphere Cultures for RNA Extraction***

Sphere cultures were pipetted from each well of the six-well plate so as not to lose cells or disturb the structure of the spheres. Each well was plated with $10^6$ cells. Since the protocol that came with the Qiagen RNEasy Kit was optimized for use with $2x10^6$ cells/sample, cells and media from two wells were pipetted into a fresh 15-mL tube to create a suspension with roughly $2x10^6$ cells/sample. Each tube of suspension was centrifuged at 1300 rpm for 4 minutes at 4º C. Media was removed from the newly-created pellet in the tube and the pellet was re-suspended in 1.0 mL of 1X HBSS. The cell-HBSS suspension was transferred to a 1.5 mL Eppendorf tube for centrifugation at 8.0 G for 5 minutes in the Accuspin Micro-centrifuge. This produced a pellet that could be used for RNA extraction.

***2.2c RNA Extraction and Reverse Transcription of cDNA***

RNA extraction from the cells was completed with the Qiagen RNeasy Mini Kit and the included protocol (Qiagen, Germantown, MD). RNA was reverse transcribed into cDNA from the Qiagen Omniscript RT Kit with the included protocol. To complete reverse transcription, oligo-dT's and Reverse Transcriptase from Invitrogen (Carlsbad, CA) and RNAse Inhibitor from New England Biosciences (Ipswich, MA) were purchased separately and used to complete the reaction. cDNA was reverse transcribed from RNA at a concentration of 100 ng/ul.

## 2.3 Quantitative Real-Time Polymerase Chain Reaction (PCR) for Juxtamembrane Isoform Expression

The expression of each of the juxtamembrane isoforms in every culture condition was quantitated with Quantitative Real-Time PCR. Primer sets to specifically amplify the Jm-a, Jm-b, Jm-c and Jm-d isoforms were optimized and validated from previously published sequences by Jesus Trevino and Kristen Richards of the Hughes Laboratory [59]. Each primer set was designed to anneal specifically to a juxtamembrane isoform of ERBB4 (see Table 2.1).

| Forward Primers (Length of Plasmid) | Sequences |
|---|---|
| **Her-4 Jm-a (9729 bp)** | 5′-CTGCACCCAAGGGTGTAACG-3′ |
| **Her-4 Jm-b (9651 bp)** | 5′-GGCCTGATGGATAGAACTCC-3′ |
| **Her-4 Jm-c (9609 bp)** | 5′-CAAACTGCACCCAAGGAACTC-3′ |
| **Her-4 Jm-d (9726 bp)** | 5′-CGGCCTGATGGATAGGTGTAAC-3′ |
| **Reverse Primer (Length of Plasmid) Common to All Isoforms** | 5′-GCAAATGTCAGACCCACAATG-3′ |

**Table 2.1 Primer Sequences Used for PCR Amplification of ERBB4 Juxtamembrane Isoforms.** From previous studies, four forward primers were used that annealed specifically to each of the ERBB4 juxtamembrane isoforms. A common reverse primer was used for amplification of all four isoforms [59]. Absolute copy number of each isoform was obtained through creating standard curves for the message of each isoform normalized to GAPDH.

Standard curves for a primer set were obtained by amplifying serial dilutions of pcDNA 3.1 plasmids with the isoform DNA. Serial dilutions of the plasmid were made from $10^9$ copies/µl to $10^2$/µl copies in 100µl of each of deionized water. A standard curve for the reference gene GAPDH was made by amplifying a 161 base-pair fragment of GAPDH. Plasmid concentration was obtained through readings on the ThermoScientific NanoDrop ND1000 Spectrophotometer (Wilmington, DE).

Plasmid sizes were 9729 base pairs for Jm-a, 9651 base pairs for Jm-b, 9609 base pairs for Jm-c and 9726 base pairs for Jm-d, respectively. Quantitative real-time PCR (qRT-PCR) was conducted in a BioRad C1000 iCycler (Hercules, CA), using BioRad iQ SYBR Green Supermix (Hercules, CA) in a 50 µl -reaction. Each reaction contained 25µl of SYBR Green,

2µl of forward primer, 2µl of reverse prime, 20µl of UltraPure DNase/RNase-Free Distilled Water (Life Technologies, Carlsbad, CA) and 1µl of cDNA reverse-transcribed at 100ng/µl. Absolute quantification of mRNA copy number was obtained by substitution of the normalized Ct value into the equation $\log_{10}(n_0)=Ct$ , where $n_0$ is absolute copy number [59].

## 2.4 Immunohistochemical Analysis of Mice Injected With ERBB4 Knockdown (KD) vs. ERBB4 Normal Control (NC) Cells

### *2.4a In Vivo Data Collection from Mice*

Two *in vivo* studies were conducted in NOD-SCID γ IL-2 deficient mice to assess the effects of ERBB4 knockdown on development of osteosarcoma metastases in lungs. Each study had six control mice and six experimental mice included in the final analysis, for a total of twelve mice in the control group and twelve mice in the experimental group. shRNA was used for ERBB4 knockdown in CCH-OS-O, a human metastatic osteosarcoma cell line. The knockdown efficiency was verified through Western blot prior to injection. The control mice were given intratibial injections of $10^6$CCH-OS-O control (NC) cells and the experimental mice were injected with $10^6$ CCH-OS-O cells with ERBB4 knockdown (KD). The experiments were analyzed separately because the scatter within experimental groups indicated that these experiments were not replicates.

Tumors were allowed to grow in the mice for eight weeks. Mice were sacrificed at this time. The tibias and lungs from each mouse were harvested and preserved in formalin, after which they were sent to the MD Anderson Histology Core for processing and embedding into paraffin blocks. The blocks were sectioned onto 0.5 micron sections and affixed to slides for staining with antibody. A set of slides were also stained for hematoxylin and eosin, a commonly-used histological stain that exhibits a variety of nuclear, cytoplasmic and extracellular matrix features [59].

### *2.4b Immunohistochemical Staining for Vimentin and ERBB4*

Slides of lung and tibial tissue from each mouse were sent to MD Anderson Science Park (Smithville, Texas) for immunohistochemical staining. Two sets of slides of adjacent sections of lung and tibial tissues were stained for each mouse. One set of slides was stained

with a rabbit polyclonal antibody against human ERBB4 (LS-A2847 from LS Bio). The second set was stained with a mouse monoclonal antibody (Abcam 8069) against human vimentin, which is used as a pathological marker for osteosarcoma. To ensure that there was no cross-reactivity with murine pulmonary tissue, a Western blot was performed by Yi Zhang of the Hughes Laboratory of CCH-OS-O, CCH-OS-D and K7M3, a metastatic murine osteosarcoma line derived from Saos2 by the laboratory of Eugenie Kleinerman in the Department of Experimental Pediatrics at MD Anderson Cancer Center.

K7M3 was kindly given to us for this experiment by the Laboratory of Eugenie Kleinerman, MD. The antibody detected vimentin in CCH-OS-O and CCH-OS-D but did not bind to vimentin in K7M3, demonstrating that the antibody was suitable for specifically detecting human osteosarcoma metastases in the experimental mice.

***2.4c Immunohistochemical Analysis of ERBB4 KD and NC Mice***

The procedure for immunohistochemical analysis was optimized to detect and quantify human osteosarcoma metastases in mouse lungs. The tibia was examined first for presence of tumor by positivity for vimentin on the vimentin antibody-stained slide and the H&E-stained slide. If there were a vimentin-positive tumor present in the tibia that was confirmed with H&E, data from that mouse was included in analyses of lung metastases. ERBB4-antibody stained slides of the tibias were checked for confirmation of ERBB4 knockdown in the KD mice and for ERBB4 expression in the NC mice.

Next, the lungs were analyzed for number and size of pulmonary metastases using the slide stained for vimentin expression and for ERBB4 immunoreactivity on the slide stained for ERBB4 expression. The ERBB4- and vimentin-stained slides, made from adjacent slices of the FFPE block, were mounted side by side on a Leica DMLS Microscope and viewed at the 4X, 10X and 40X magnifications to gain as complete a count as possible of the osteosarcoma

metastases within the lung. The slide stained for vimentin would be checked first for specific detection of osteosarcoma lung metastases. We attempted to get as accurate a picture as possible of the metastatic burden in each mouse by counting the total number of metastases expressing vimentin and categorizing them by size. After the metastases were quantified and categorized in one section of lung, the same section of lung would be examined on the ERBB4-stained slide for ERBB4 immunoreactivity in those lesions. Lesions with at least one viable ERBB4-positive cell were designated as "ERBB4-positive." Those lesions with absolutely no expression of ERBB4 in any cell were designated "ERBB4-negative." To confirm that each ERBB4-positive lesion was indeed an osteosarcoma metastasis, the slide stained for vimentin was onstage with the slide stained for ERBB4 expression to see if there was a corresponding lesion on the slide stained with vimentin. Metastases were categorized by size in microns and number of cells, as shown in Table 2.2. Vimentin-positive lesions were independently verified as osteosarcoma of oligometastases at the Department of Pathology at MD Anderson Cancer Center.

| | |
|---|---|
| **Macrometastases** | ≥ 200 microns |
| **Micrometastases** | 6 cells-200 microns |
| **Oligometastases** | 1-5 cells |

**Table 2.2: Categorization of osteosarcoma metastases by size.** Staining with vimentin of adjacent sections of lungs showed abundant lesions of one to five cells in size in the lungs of mice injected with ERBB4 KD or NC cells at higher magnifications (10X and 40X, Leica DMLS Microscope). These metastases were designated as oligometastases because they were osteosarcoma metastases but not yet overt, like micrometastases or macrometastases at 4X. Designating the oligometastases as a separate category allowed us to see where ERBB4 may have influenced metastatic progression.

## 2.5 Statistics

Statistical analyses were conducted using GraphPad Prism6 Software. Ordinary one-way ANOVA with Tukey's Multiple Comparisons Test was used to compare significance in PCR data. The Student's paired t-test was used to compare significance in immunohistochemical data

for each experiment. Microsoft Excel 2010 was used to make graphs and scatterplots to show data variance in the immunohistochemical data.

# Chapter 3: Results

## 3.1 Changes in ERBB4 Juxtamembrane Isoform Expression with Increased Matrix and Loss of Anchorage-Independence

### *3.1a Rationale and Hypothesis*

Data from the Hughes laboratory showed by Western Blot that there was up-regulation of ERBB4 protein from monolayer cultures to sphere cultures of primary osteosarcoma cell lines, where cells spontaneously formed viable tumor spheres in anchorage-independent culture conditions (see Figure 1.4). Up-regulation of total ERBB4 protein was also observed by Western blot in neuroblastoma and post-treatment Ewing's sarcoma cell lines from monolayer to sphere cultures [51-53]. Increased expression of Jm-a Cyt-1 and Jm-a Cyt-2 isoforms was observed by qRT-PCR assays in sphere cultures from monolayer cultures of post-treatment Ewing's sarcoma cell lines, with no detectable expression of the Jm-b isoform [53].

Up-regulation of ERBB4 was also observed in "high-density" cultures of neuroblastoma and osteosarcoma, in which cells were allowed to grow to over-confluence [52]. Tumor spheres possess more highly developed cell-cell contact than cells in monolayer culture. The increased cell-cell interactions present within tumor spheroids and the up-regulation of ERBB4 expression in cells with enhanced matrix interactions in high density raised the possibility that ERBB4 may be up-regulated to aid in survival of conditions of increased cell-cell contact or matrix formation [52].

Previous studies of ERBB4 expression and signaling in primary osteosarcoma cell lines showed ERBB4 protein was primarily expressed as an 80-kDa fragment as assessed by Western Blot [75]. Immunohistochemistry on formalin-fixed paraffin blocks made from those cell lines showed that ERBB4 expression was nuclear in those cell lines [75]. Cleavable juxtamembrane ERBB4 isoforms are implicated in promoting anchorage-independent growth in both normal and malignant tissues [44]. Overexpression of Jm-a Cyt2 enhances anchorage-independent

growth and proliferation in fibroblasts and ER-positive breast cancer [48, 58]. Taken together, we hypothesized that there would be an increase in the expression of the cleavable juxtamembrane isoforms Jm-a and Jm-d from monolayer to sphere cultures of primary osteosarcoma cell lines.

The aim of this study was to assess whether juxtamembrane ERBB4 isoform expression changed with increasing culture density and anchorage independence. **We hypothesized that an increased proportion of cleavable juxtamembrane ERBB4 isoform mRNA transcript would be observed as osteosarcoma cells were grown in conditions of increasing culture density, with the greatest increase in proportion being observed in anchorage-independent culture.** We used quantitative RT-PCR (qRT-PCR) with isoform-specific primers to measure the expression levels of the four ERBB4 juxtamembrane isoforms of in monolayer, high density and anchorage-independent culture

The cleavable isoforms of ERBB4 are the Jm-a and Jm-d isoforms and the non-cleavable isoforms are the Jm-b and Jm-c isoforms. There was a significant increase in the proportion of Jm-a expressed from monolayer to sphere cultures in Saos2 and CCH-OS-O ($p < 0.05$). There was significant up-regulation of total ERBB4 transcript from monolayer to sphere culture in CCH-OS-D that was comprised primarily of an increase in Jm-a transcript. There was a significant increase in the proportion of Jm-d expressed from monolayer to sphere cultures of Saos2 ($p < 0.05$). There was significant up-regulation in Jm-d expression in CCH-OS-K ($p < 0.05$). The trend in the data shows that an increase, either in proportion or total expression, of a cleavable ERBB4 isoform may occur to enhance survival of osteosarcoma cells in anchorage-independent conditions.

### *3.1b Quantitative Real-Time PCR of Juxtamembrane Isoforms of ERBB4 in Increasing Culture Density*

Four human osteosarcoma cell lines, CCH-OS-D, Saos2, CCH-OS-O and CCH-OS-K, were selected for this study because they formed viable tumor spheroids in anchorage-independent culture and displayed up-regulation of ERBB4 from monolayer to sphere culture in anchorage-independent cultures. Each cell line was cultured in three conditions to test the effects of cell-cell contact and anchorage-independence on ERBB4 juxtamembrane isoform expression (see Figure 3.1). The first condition was conventional monolayer (MN) culture, from which cells displayed minimal contact on the plate, or 70% confluency in the case of Saos2. The second condition was "high density" (HD) culture, in which cells were allowed to grow past confluence. Contact inhibition was observed in HD cultures of Saos2. CCH-OS-D, CCH-OS-O and CCH-OS-K did not display contact inhibition even at complete confluence. The HD condition could be considered an intermediate in cell-cell contact between the monolayer and sphere cultures. The third condition was "sphere culture," or anchorage-independent culture (SP) in which cells from all cell lines formed tumor spheroids. Quantification of each juxtamembrane isoform was conducted with isoform-specific quantitative RT-PCR for cells grown in the three culture conditions. One-way ANOVA with multiple comparisons correction was performed on each data set to compare differences between means.

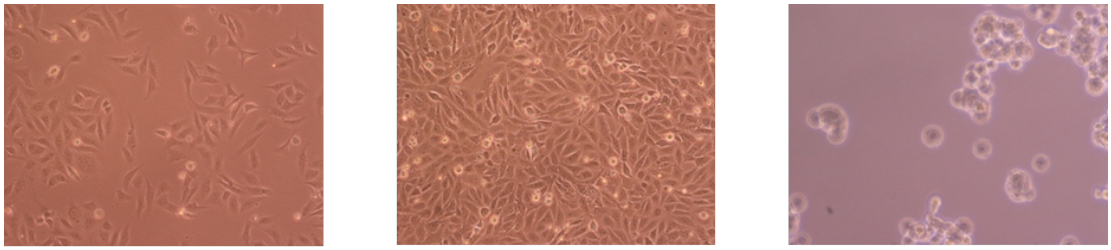


**Figure 3.1: Microscopy of culture conditions in cell line CCH-OS-O**. These panels show microscopy of cell cultures of CCH-OS-O, a human-derived osteosarcoma cell line. (A) Conventional monolayer culture CCH-OS-O, in which cells were harvested before reaching confluence. (B) A high-density condition was included in the experiment to test the effects of cell-cell contact on ERBB4 up-regulation in osteosarcoma. (C) CCH-OS-O was picked for its ability to survive in anchorage-independent culture by cells spontaneously forming small 3-D aggregates of viable cells called tumor spheroids. CCH-OS-O tumor spheroids showed up-regulation of total ERBB4 protein by Western blot. Since all cell lines selected for this experiment demonstrated anchorage-independent survival as tumor spheroids with ERBB4 up-regulation, it was hypothesized that there may also be increased transcription of cleavable juxtamebrane ERBB4 isoforms with increased cell-cell contact.

### 3.1c Increases in expression of cleavable juxtamembrane ERBB4 isoform expression are important in anchorage-independent osteosarcoma cultures

Isoform expression was first examined in each cell line for up-regulation of absolute transcript number in response to changes in culture conditions. There is a significant up-regulation of Jm-a from monolayer to sphere culture in CCH-OS-D (see panel A, Figure 3.2), which primarily underlies the up-regulation of total ERBB4 transcript when examining changes in absolute mRNA copy number from monolayer to sphere cultures in CCH-OS-D. CCH-OS-D is a primary osteosarcoma cell line which was derived from a post-treatment tumor, which agrees with data that shows up-regulation of Jm-a transcript in post-treatment Ewing's sarcoma tumor spheroids [53]. The data for the Jm-d isoform (see panel A, Figure 3.3) shows a significant increase of Jm-d isoform from monolayer to high density cultures and monolayer to sphere cultures ($p < 0.05$). There is a decrease of Jm-d expression from high density to sphere culture, which is non-significant.

Saos2 displayed a significant increase in proportion of Jm-a and Jm-d from monolayer to sphere cultures (see panel B, Figures 3.2 and 3.3 respectively) ($p < 0.05$). When absolute

transcript numbers for all four isoforms are totaled for each culture condition and compared across conditions in Saos2, we see that the absolute levels of all four transcripts added together are approximately equal between high density and sphere cultures with a modest, non-significant increase in total ERBB4 transcript from monolayer to high density cultures. There is a significant increase in the proportion of Jm-a and Jm-d expressed from monolayer to sphere culture and high density to sphere cultures ($p < 0.05$). Interestingly, the increase in total ERBB4 transcript seen from monolayer to high density cultures is due to increases in Jm-b and Jm-c transcript levels that did not reach significance (see Panels B, Figures 3.4 and 3.5 respectively). Jm-c and Jm-d are often expressed together in tissues. There is a proportionate increase in Jm-d ($p < 0.05$) with accompanying proportionate decrease in Jm-c from high density to sphere culture in Saos2. Jm-b is the predominant isoform expressed in Saos2 in monolayer culture. Jm-b and Jm-c are the two highly up-regulated isoforms from monolayer to high density cultures but there is a significant increase in proportion from non-cleavable (Jm-b/Jm-c) to cleavable (Jm-a/Jm-d) expression from high density to sphere culture ($p < 0.05$), making Jm-a and Jm-d the isoforms with the highest absolute copy number in sphere cultures of Saos2.

Changes in cell-cell contact significantly affected the proportion of isoforms expressed in CCH-OS-O though the absolute copy number stayed roughly equal across culture conditions. There is a an increase in Jm-a copy number (see panel C, Figure 3.2) with accompanying decrease in Jm-b, Jm-c and Jm-d isoforms (see panels C, Figures 3.3-3.5) that total to slightly lower copy number than the increase in Jm-a from monolayer to sphere culture in CCH-OS-O ($p < 0.05$). There is a significant increase in Jm-a expression from high density to sphere culture in CCH-OS-O but significant decreases in expression occur from monolayer to high density culture in Jm-b, Jm-c and Jm-d ($p < 0.05$). Taken together, this data indicates that Jm-a may be up-regulated while the other juxtamembrane isoforms may be down-regulated in CCH-OS-O.

This could account for the proportionate increase in Jm-a expression from monolayer to sphere culture and significant increase from high density to sphere culture and the proportionate decrease in expression of Jm-b, Jm-c and Jm-d from monolayer to sphere culture in this cell line.

CCH-OS-K will be discussed in a separate section due to its derivation from a malignant pleural effusion. CCH-OS-D, Saos2 and CCH-OS-D are primary osteosarcoma cell lines and can thus be discussed together. In sphere cultures of these cell lines, cleavable isoforms were the predominant isoforms expressed in sphere cultures. CCH-OS-D up-regulated the Jm-a isoform, as seen by the significant increase in Jm-a transcript number from monolayer to sphere culture compared to transcript numbers of other isoforms. In Saos2, the total isoform expression increased from monolayer to high density cultures but there were significant increases in the proportion of Jm-a and Jm-d isoforms from high density to sphere cultures. CCH-OS-O increased the proportion of Jm-a expressed while decreasing the proportion of the other three isoforms expressed from monolayer to sphere cultures, suggesting that Jm-a may be the biologically relevant isoform in CCH-OS-O. The trend of the data indicates that an increase in cleavable isoform expression, by proportion or overall transcription, is important to survival when transitioning from adherent to anchorage-independent cultures in primary osteosarcoma cell lines.

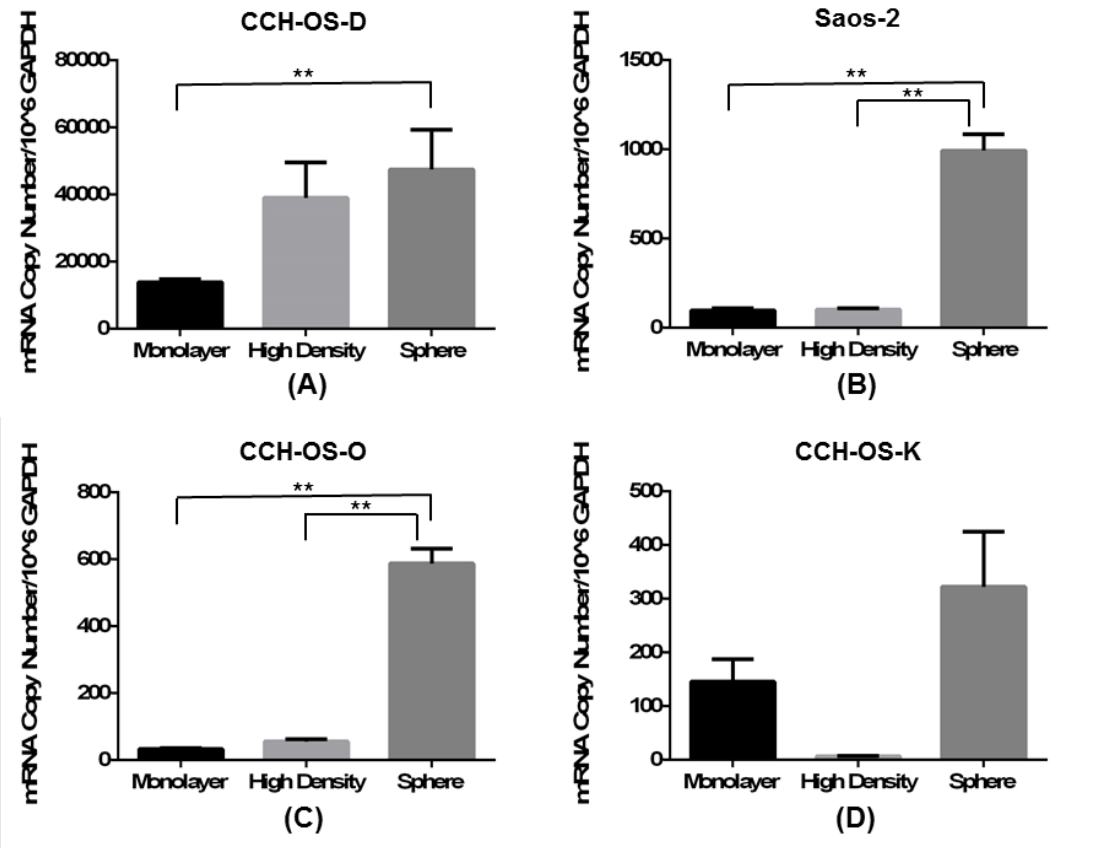


**Figure 3.2: The proportion of cleavable juxtamembrane isoform Jm-a expressed increases from monolayer to anchorage-independent culture in a majority of osteosarcoma cell lines.** (A) CCH-OS-D shows a significant increase in expression of isoform Jm-a from monolayer to sphere culture. (B) Saos2 shows a significant increase in expression of Jm-a from monolayer to high density culture and high density to sphere culture. (C) CCH-OS-O shows a significant increase in expression of Jm-a from monolayer to high density culture and high density to sphere culture. CCH-OS-O and Saos2 showed a significant increase in Jm-a isoform transcript number with increasing density, which suggests that ERBB4 transcription is significantly increased in response to increasing cell-cell contact where basal ERBB4 expression is low. (D) There was no significant increase from monolayer to high density or high density to sphere in Jm-a transcript in CCH-OS-K but CCH-OS-K also showed the most robust expression of ERBB4 Jm-d transcript of any cell line, which may indicate that CCH-OS-K predominantly expressed Jm-d transcript as its cleavable isoform. There is also an increase in copy number of all juxtamembrane isoform transcripts of ERBB4 in CCH-OS-K from monolayer to sphere culture, which may mean that total ERBB4 transcription in CCH-OS-K may be up-regulated to survive anchorage-independent conditions.

**$p < 0.05$.

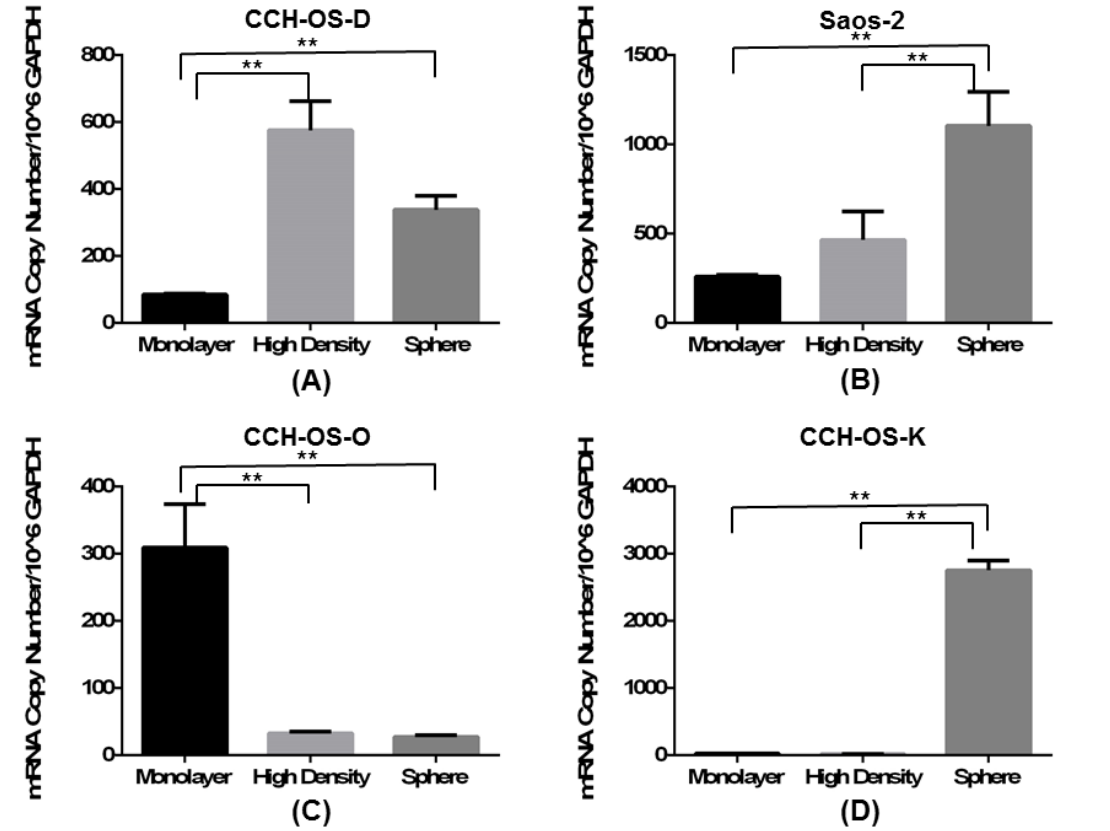


**Figure 3.3: The proportion of cleavable juxtamembrane isoform Jm-d expressed increases from monolayer to anchorage-independent culture in a majority of osteosarcoma cell lines.** (A) There is an increase in Jm-d transcript from monolayer to sphere culture and from monolayer to high density culture, which suggests that increased cell-cell contact may be directly up-regulating transcription of Jm-d isoform in CCH-OS-D. (B) There is an increase in Jm-d transcript from monolayer to sphere and high density to sphere cultures in Saos2, which means that a direct effect of cell-cell contact on Jm-d transcription in Saos2 may be mediated by greater density or factors that lead more specifically to anoikis resistance. (C) There is an increase in Jm-d transcript from monolayer to sphere and high density to sphere cultures in CCH-OS-O, which means that a direct effect of cell-cell contact on Jm-d transcription in CCH-OS-O is difficult to establish without further experiments. (D) Jm-d transcript number from monolayer to sphere culture and high density to sphere culture shows the greatest increase in proportion of all cell lines in CCH-OS-K. All juxtamembrane isoforms of ERBB4 displayed increased number of transcript from monolayer to sphere cultures, suggesting that total ERBB4 transcription may be up-regulated to mediate survival of tumor spheroids in CCH-OS-K

**$p < 0.05$

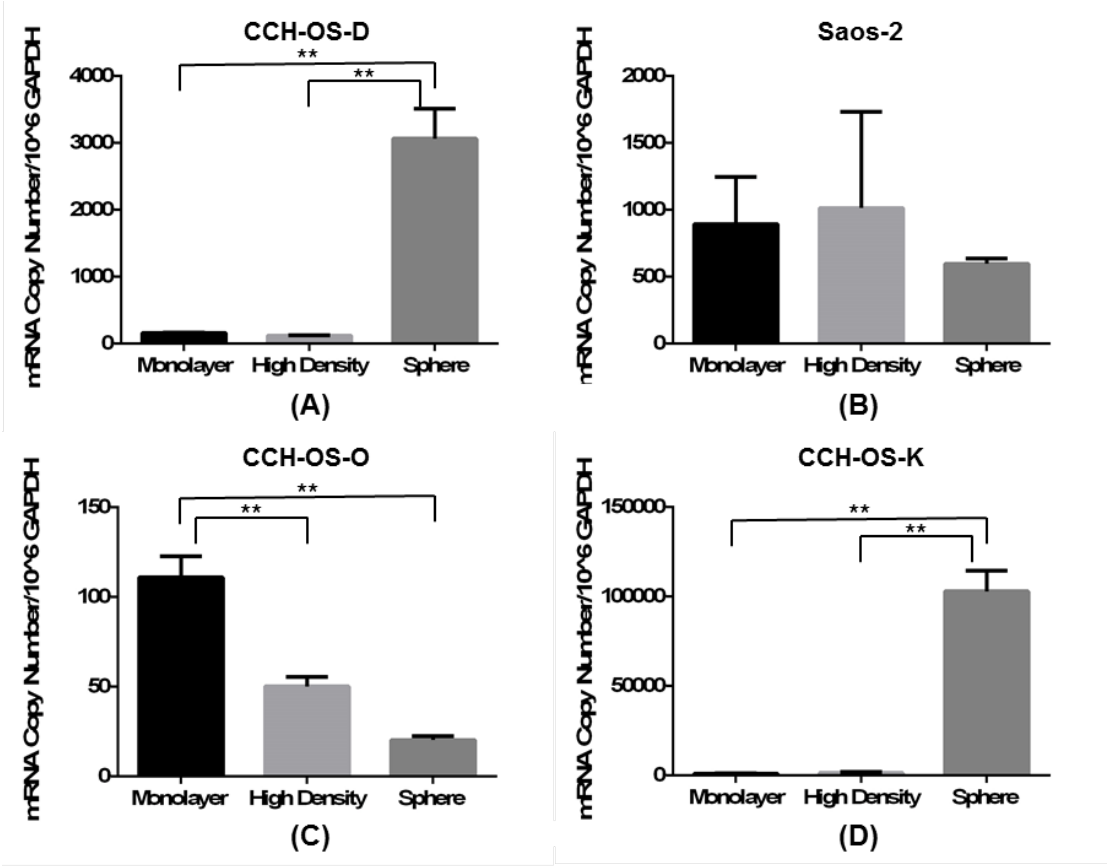


**Figure 3.4: The proportion of non-cleavable juxtamembrane isoform ERBB4 Jm-b is expressed in proportion to cleavable juxtamembrane isoform Jm-a in a majority of OS cell lines.** (A) CCH-OS-D shows a total up-regulation in Jm-b isoform transcript in sphere culture from monolayer to sphere culture and high density to sphere culture. (B) The expression of Jm-b transcript in Saos2 decreases in proportion to the increase in Jm-a isoform expression (see Figure 3.2) from high density to sphere culture. Jm-a and Jm-b are thought to be co-expressed together as cleavable and non-cleavable isoform in many tissues. The differences in culture conditions in Saos2 were statistically insignificant. (C) CCH-OS-O is the only cell line to show a density-dependent up-regulation in Jm-b transcript from monolayer to high density cultures but also displays up-regulation of Jm-b transcript from monolayer to sphere culture, which suggests that increased cell-cell contact itself does up-regulate Jm-b transcript in CCH-OS-O. (D) CCH-OS-K shows a total up-regulation in Jm-b isoform from monolayer to sphere culture and high density to sphere culture. All juxtamembrane isoforms of ERBB4 displayed increased number of transcript from monolayer to sphere cultures, suggesting that total ERBB4 transcription may be up-regulated to mediate survival of tumor spheroids in CCH-OS-K.

**$p < 0.05$

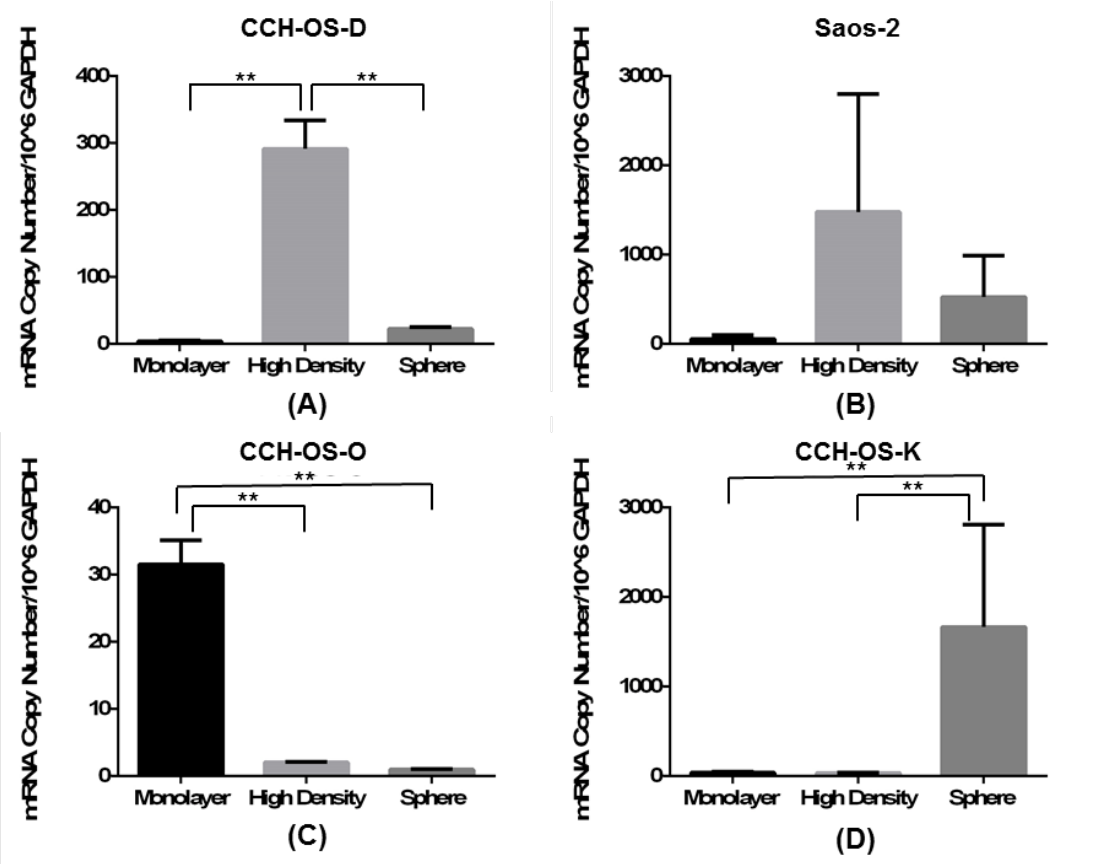


**Figure 3.5: Expression of the Jm-c isoform in osteosarcoma cell lines..** (A) There is an increase in the proportion of Jm-c isoform expressed in CCH-OS-D from monolayer to high density and a decrease in expression from high density to sphere that is proportional to the increase in Jm-d (see Figure 3.3). (B) Saos2 shows an increase from monolayer to high density culture but it decreases in proportion to the increase in Jm-d isoform expression from high density to sphere cultures of Saos2 (see Figure 3.3). (C) CCH-OS-O shows a decrease in proportion of Jm-c transcript from monolayer to high density culture and high density culture to sphere culture. (D) CCH-OS-K shows significant up-regulation of Jm-c isoform from monolayer culture to sphere culture, which points to an up-regulation of all juxtamembrane isoforms of ERBB4 in response to increased cell-cell contact.

** $p < 0.05$

### *3.1d Patterns in non-cleavable isoform expression do not show consistent trends with increased cell-cell contact or anchorage-indepdendence*

The absolute quantification of mRNA copy numbers of the Jm-b and Jm-c isoforms for all cell lines are shown in Figure 3.4 and Figure 3.5. Data shows that the Jm-a/Jm-b isoforms and Jm-c/Jm-d isoforms are frequently co-expressed in tissues, which formed the basis for the comparisons in Figures 3.6 and 3.7 [12]. The expression of the Jm-b and Jm-c isoforms will be compared first by culture conditions. We had included the high density condition because previous data had shown up-regulation of ERBB4 protein in high density cultures of neuroblastoma and osteosarcoma. The high density condition introduces some of the stressors associated with metastasis such as reduced access to nutrients and oxygen, increased cell-cell contact and crowding and loss of contact inhibition. The Jm-b and Jm-c isoform data highlight that high density and sphere cultures were not an adequate means of comparison for attempting to answer if increased cell-cell contact affected ERBB4 transcriptional levels or alternate splicing.

CCH-OS-K will be discussed in the following section because of its origin as a malignant pleural effusion; its inclusion with the other cell lines derived from primary tumors would present major confounds to data interpretation. To start, the data from CCH-OS-O agreed with our initial hypothesis. Jm-b and Jm-c expression decreased from monolayer to high density and monolayer to sphere culture ($p < 0.05$). Along with the decrease in the cleavable Jm-d isoform, the decreases in Jm-b and Jm-c expression were proportionate to the increase in Jm-a expression from monolayer to sphere cultures (see Figure 3.7). The isoform with the absolute copy number that renders the decrease proportionate from monolayer to sphere is is Jm-d, however.

CCH-OS-D shows significant up-regulation of the Jm-b isoform from monolayer to sphere culture ($p < 0.05$). While there is an almost ten-fold difference between the copy numbers of the Jm-a and Jm-b isoforms in sphere culture, the copy number of Jm-b is almost ten-fold higher than the copy number of Jm-d. Jm-d expression was significantly increased from monolayer to sphere and monolayer to high density ($p < 0.05$) but decreased from high density to sphere culture. Jm-c showed an increase from monolayer to high density but a decrease from high density to sphere culture with both trends reaching significance ($p < 0.05$). The decrease in Jm-c from high density to sphere was proportionate to the decrease in Jm-d from high density to sphere. The similar trends in Jm-a/Jm-b and Jm-c/Jm-d expression levels (see Figure 3.6) between culture conditions provides further support for looking at juxtamembrane isoforms Jm-a/Jm-b and Jm-c/Jm-d in terms of co-expression in osteosarcoma cell lines. It also made us reassess if high density and sphere cultures were more biologically dissimilar than similar.

Jm-b and Jm-c expression in Saos2 showed an up-regulation of both isoforms from monolayer to high density culture but a significant decrease in their proportions expressed from high density to sphere culture ($p < 0.05$). There is a significant increase in the proportion of in Jm-a and Jm-d expressed from high density to sphere culture in Saos2 ($p < 0.05$). Figure 3.6 illustrates the shift in proportion from non-cleavable isoforms from high density to sphere cultures and the up-regulation of the non-cleavable isoforms from monolayer to high density cultures. In effect, the data from the high density condition showed that the high density culture is not an intermediate between monolayer and sphere cultures in osteosarcoma. This will be elaborated on further in the discussion.

### *3.1e CCH-OS-K could be a better model for osteosarcoma survival in anchorage-independent conditions*

CCH-OS-K was derived from a malignant pleural effusion of a patient [78]. To survive the circulation and reach a distant site such as the pleura, osteosarcoma cells must have acquired mechanisms to survive various stressors. One such stressor is loss of attachment to ECM, which we simulated with our tumor sphere culture [71]. Unlike the other cell lines in our experiment that were derived from primary tumors, CCH-OS-K had already initiated programs to survive the loss of matrix attachment. Thus, CCH-OS-K may serve as a better model for understanding the roles of ERBB4 expression in anchorage-independent survival in osteosarcoma.

Up-regulation of all four isoforms from monolayer and high density cultures to sphere culture was observed, with significant up-regulation of Jm-b, Jm-c and Jm-d ($p < 0.05$). Among all the culture conditions in our experiment, the highest absolute ERBB4 mRNA copy number was observed in sphere cultures of CCH-OS-K (see Panels C and D, Figure 3.7). That total was comprised primarily by expression of Jm-b. There was significant up-regulation of Jm-d in sphere cultures but its expression was approximately 50-fold less than that of Jm-b in spheres ($p < 0.05$). This is still consistent with the data from primary osteosarcoma cell lines that showed cells significantly increasing the expression of at least one cleavable isoform from monolayer to sphere culture. The increase in Jm-b expression from adherent to non-adherent conditions (monolayer and high density to sphere) could indicate that expression of other isoforms may vary in response to the stressors at different stages of disease progression. PCR assays to measure isoform expression in other cell lines of similar origin would have to be performed to draw larger conclusions from these results.

### *3.1f Summary*

There was a significant increase in cleavable (Jm-a/Jm-d) isoform expression, either by proportion or total up-regulation, from monolayer to sphere cultures in all of the cell lines in our experiment ($p < 0.05$). It was difficult to see trends in the data for the high density culture condition and subsequently, the non-cleavable isoforms because of our using the high density culture as an intermediate in cell-cell contact between monolayer and sphere cultures when it is biologically quite different from both culture conditions. A more extensive treatment of the biological features that we did not fully consider when including the high-density condition will be included in the discussion section of the thesis. Finally, CCH-OS-K was derived from a malignant pleural effusion, or cells that had survived loss of attachment *in vivo.* We saw significant up-regulation of cleavable Jm-d but the most up-regulated isoform was Jm-b, with up-regulation levels that made its absolute mRNA expression highest of all the conditions in our experiment.

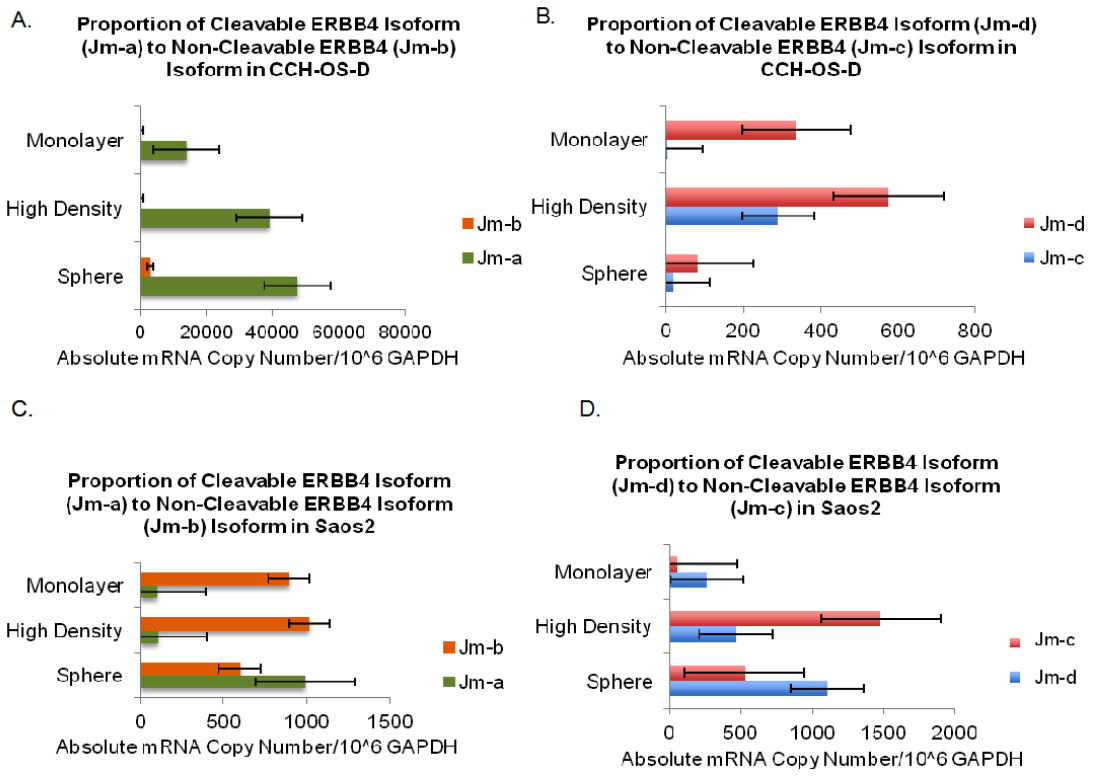


**Figure 3.6: The proportion of cleavable juxtamembrane isoforms expression increases from monolayer to sphere cultures in CCH-OS-D and Saos2.** (A) There is increase in proportion of the cleavable Jm-a isoform of ERBB4 from monolayer to sphere cultures of CCH-OS-D, with an increase of the non-cleavable Jm-b isoform from monolayer to sphere culture as well. (B) The absolute copy numbers of Jm-c and Jm-d isoforms show that there is a proportionate increase in cleavable Jm-a and Jm-d isoforms and proportionate decrease in non-cleavable Jm-b and Jm-c isoforms from monolayer to sphere cultures. The difference is obscured in CCH-OS-D due to the relatively low absolute copy numbers of the Jm-c and Jm-d isoforms. (C) Saos2 shows an increase in the proportion of Jm-b isoform from monolayer to high density culture relative to Jm-a but there is a proportional increase in Jm-a and decrease in Jm-b from high density to sphere culture. (D) We see an up-regulation of the Jm-c and Jm-d isoforms in Saos2 from monolayer to high density culture and that the proportion of Jm-d increases and Jm-c decreases from high density to sphere culture. Cumulatively, there is up-regulation of all of the ERBB4 isoforms from monolayer to high density culture but there is a proportionate increase of the cleavable (Jm-a/Jm-d) isoforms and proportionate decrease of the non-cleavable (Jm-b/Jm-c) isoforms from high density to sphere culture, which could indicate that cleavable juxtamembrane isoforms are up-regulated proportionally in conditions where increased cell-cell contact is critical to tumor cell survival.

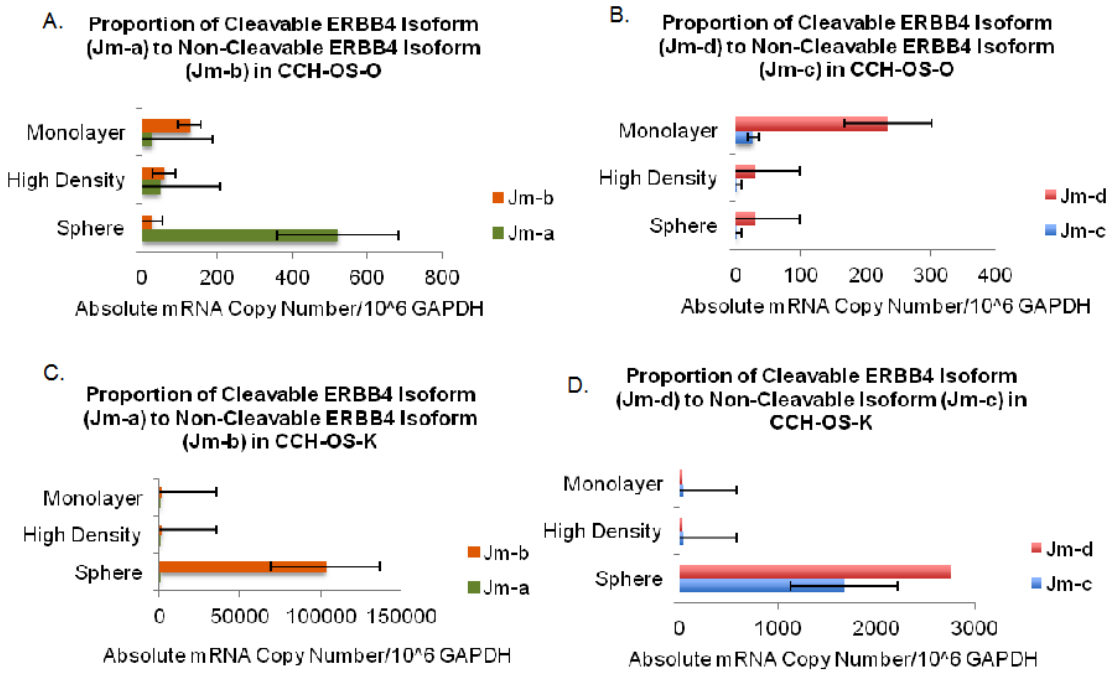


**Figure 3.7: The proportion of cleavable juxtamembrane isoform Jm-a increases proportionally from monolayer to sphere culture of CCH-OS-O, with Jm-b as the predominant isoform in sphere culture in CCH-OS-K.** (A) There is significant up-regulation of Jm-a transcript ($p < 0.05$) from monolayer to sphere culture. (B) The absolute copy numbers of Jm-c and Jm-d isoforms decrease proportionally to the increase in Jm-a transcript from monolayer to high density to sphere culture. This decrease is seen in combination with the decrease in Jm-b transcript from Figure 3.7A, showing that all isoforms are down-regulated in sphere culture with a proportionate increase in Jm-a. Total transcript number of all juxtamembrane isoforms is approximately the same between monolayer and sphere cultures of CCH-OS-O. (C) CCH-OS-K up-regulates the Jm-b transcript from monolayer to sphere culture in such high proportion relative to the other isoforms that it may be considered that CCH-OS-K up-regulates the Jm-b isoform to possibly enhance its survival in conditions of increased cell-cell contact. (D) There is up-regulation of the Jm-c and Jm-d isoforms in CCH-OS-K as well. The up-regulation of Jm-b is 33-fold above that of Jm-d and 50-fold above Jm-c, suggesting that Jm-b may play the critical role for ERBB4 signaling in CCH-OS-K.

## 3.2: Immunohistochemistry of ERBB4 Expression in Lung Metastases with ERBB4 Knockdown and Control CCH-OS-O Cells

### *3.2a Rationale and Hypothesis*

We hypothesized that ERBB4 was a mediator of osteosarcoma metastasis due to ERBB4 expression enhancing survival in conditions that are necessary for metastatic spread. ERBB4 up-regulation enhances cells' ability to withstand stressors that would normally limit metastasis such as anoikis, serum starvation and chemotherapy [52]. ERBB4 knockdown in neuroblastoma cells reduced anchorage-independent survival and increased apoptosis in single cells and tumor spheres [52]. Across a tissue microarray of patient-derived osteosarcoma samples from the Hughes laboratory (Figure 3.8, unpublished data) stained for expression of EGFR, ERBB2 and ERBB4, staining intensity was elevated from primary tumors to lung metastases for all three receptors but ERBB4 expression was most elevated in staining intensity.

The experiments in section 3.1 showed that the absolute mRNA copy number of at least one of the cleavable isoforms of ERBB4 (Jm-a/Jm-d) increases significantly, by proportion or through up-regulation, from monolayer to sphere cultures in osteosarcoma cell lines CCH-OS-D, Saos2, CCH-OS-O and CCH-OS-K ($p < 0.05$). Previous findings showed primarily nuclear immunoreactivity when staining archival osteosarcoma tumor samples for ERBB4 expression [75]. Taken with the PCR data, we thought immunohistochemical staining for ERBB expression would show us if ERBB4 localized to the nucleus and signaled through proteolytic cleavage in osteosarcoma cells.

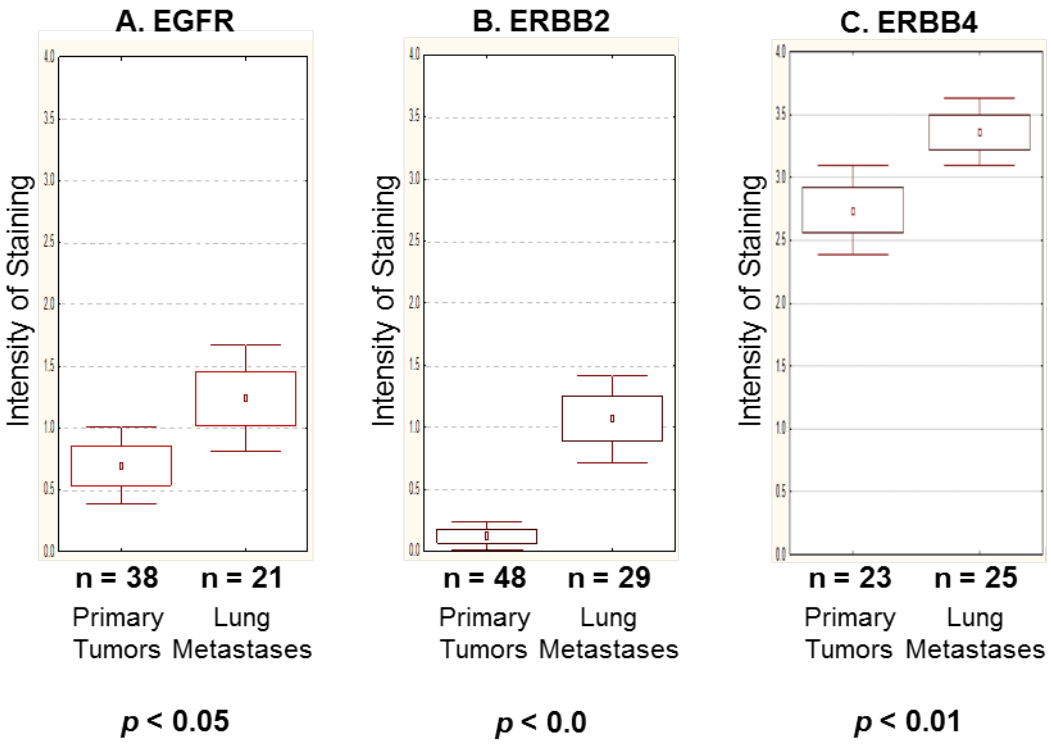


**Figure 3.8: Expression of ERBB Receptor Tyrosine Kinases increases in osteosarcoma metastases from primary tumors.** The data above is taken from a tissue microarray (TMA) constructed from patient-derived material. (A) EGFR staining intensity is elevated significantly from primary tumors to metastases. (B) ERBB2 staining intensity is elevated significantly from primary tumors to metastases. (C) There is a significant increase in ERBB4 staining in lung metastases from primary tumors. Source: TMA constructed at the University of Michigan, staining perfomed in the Hughes Laboratory (Department of Experimental Pediatrics, MD Anderson Cancer Center, Houston, TX), reading by Dr. Wei-Lien Wang (Department of Pathology, MD Anderson Cancer Center, Houston, TX).

Our aim with this experiment was to use immunohistochemical staining to understand if ERBB4 expression was necessary for osteosarcoma metastasis and if so, where it was localized in the cell. We used immunohistochemistry to study ERBB4 expression in the primary tumors and lung metastases of mice that were injected with CCH-OS-O cells with ERBB4 knockdown and CCH-OS-O scrambled control cells. **Our aim was to see if knockdown of ERBB4 affected the formation of gross osteosarcoma metastases in the lung.** To achieve that aim, we stained from each lung one section with an antibody against ERBB4 and an adjacent section from the same lung with an antibody against vimentin, an intermediate filament protein that is used as a pathological marker for osteosarcoma.

Staining adjacent slides for vimentin verified the presence of metastases that were 1-5 cells in size that were ERBB4-negative and that had been difficult to distinguish as metastases

by examining H&E stains alone due to their size. ERBB4 expression did not affect the establishment of metastases ranging from one to five cells in size but ERBB4 knockdown resulted in significant reduction of micrometastases (6 cells-200 microns) and macrometastases (> 200 microns) ($p < 0.05$).

***3.2b Quantification of ERBB4-positive osteosarcoma metastases***

We wished to see if knockdown of ERBB4 affected the formation of gross osteosarcoma metastases in the lung by comparing the numbers of metastatic lesions in the lungs of mice injected with CCH-OS-O cells with short hairpin RNA (shRNA) against ERBB4 and mice injected with CCH-OS-O scrambled control shRNA cells. The specimens used for this study were collected from two *in vivo* experiments, each containing six experimental and six control mice. Mice were included if they had a tibial tumor on H&E section that stained positive for vimentin.

To assess the efficacy of our knockdown prior to injection, ERBB4 expression was measured in CCH-OS-O cells with ERBB4 knockdown and scrambled control cells by Western Blot. Our blot showed a knockdown efficiency of 99%. We also stained a tibial section for every mouse included in the data set for ERBB4 expression as an added control to ensure that there was no detectable ERBB4 expression in the tibias of the mice in the knockdown group.

Analysis of lung sections of ERBB4-stained knockdown and control mice displayed what seemed to be metastases of one to five cells scattered variably across the sections.We initially suspected that these were artifacts from staining or slide preparation because of the weak ERBB4-positivity of these cells. The presence of these apparent lesions with variable ERBB4-positivity demonstrated the need for a stain that would reliably detect total osteosarcoma metastases regardless of ERBB4 expression.

Vimentin is used as a pathological marker to establish a clinical diagnosis of osteosarcoma, regardless of subtype. Since vimentin expression is a defining feature of osteosarcoma cells, we stained a second set of slides of adjacent sections of the tibia and lung of each mouse with a human-specific vimentin antibody. Members of the Hughes laboratory collaborated to test the specificity of the antibody by performing a Western blot on a panel of human cell lines CCH-OS-O and CCH-OS-D with a metastatic mouse osteosarcoma line K7M3 included as a control. Vimentin was detected only in the human cell lines, which ensured that this this antibody was specific for human osteosarcoma metastases in mouse lungs. The Western blot could not be included in this thesis due to a missing beta-actin control but the experiment will be replicated in the future to further this work.

Two sets of slides from the lung and tibia from each animal were analyzed. One set was of slides of tibia and lung stained with the vimentin antibody and the other set were slides of adjacent sections of tibia and lung stained with the ERBB4 antibody. The slides were mounted next to each other on the microscope stage and viewed at magnifications of 4X, 10X and 40X to obtain total counts of metastases using vimentin positivity. Next, we assessed expression patterns on the ERBB4-stained slides. A primary tumor or metastasis was defined as "ERBB4-positive" if it contained at least one viable cell that was immunoreactive for ERBB4 and corresponded to a lesion where all cells within the lesion expressed vimentin. A lesion was designated "ERBB4-negative" if it was vimentin-positive and we could not detect any ERBB4-positive cells.

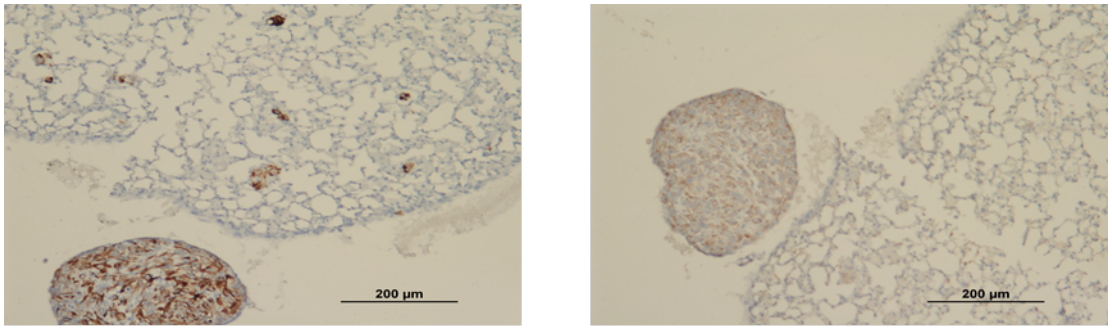


**Figure 3.9: Staining for vimentin shows the presence of oligometastases.** The above figures are of adjacent sections of lung from a mouse injected with CCH-OS-O NC cells. (A) Staining with vimentin shows metastases that were not detectable previously at 10x magnification. Metastases ranging from one to five cells were found throughout lungs of mice in the experimental and control conditions and were categorized as oligometastases. (B) shows the adjacent section of lung stained for ERBB4. There is a grossly detectable lesion that stains positive for ERBB4 but there are no ERBB4-positive oligometastases. The staining with vimentin in (A) shows that ERBB4 may not be necessary for survival of the metastatic cascade in osteosarcoma cells but that it may be critical to metastatic progression.

### *3.2c Seeding of oligometastases is not correlated to ERBB4 expression in oligometastatic lesions*

Data from the two experiments were analyzed separately, as they could not be considered replicates for reasons that will be expanded upon in the discussion. The approximately equal numbers of oligometastases in the lungs of ERBB4 KD and NC mice led us to consider that ERBB4 expression may be important later in the metastatic cascade for osteosarcoma cells, such as when seeded cells in the lungs progress to detectable metastatic lesions. The variability in size of metastases and their ERBB-positivity led us to count metastases and categorize them by size (see Figure 3.9). Categorization by size was performed to see if it would provide "proof of principle" that ERBB4 expression becomes critical during metastatic progression for osteosarcoma. We expected to see a significant decrease in macrometastases and micrometastases. Macrometastases were detectable by visual inspection (> 200 microns) and micrometastases were usually visible at 5X or by 10X if they were as small as 6 cells. Oligometastases represented "micrometastatic" disease in patients, metastases that did not pass the threshold of detection by CT imaging. By microscope, these were lesions that were

detectable only at 40X magnification. Figure 3.10 shows the total counts of oligometastases for the ERBB4 NC and KD groups in Experiment 1 and Figure 3.11 shows the total counts of oligometastases for the ERBB4 NC and KD groups in Experiment 2. Experiment 1 was conducted in June 2011 and Experiment 2 in August 2011, hence their designations.

The mean + SEM for the ERBB4 NC group (n = 6) was 503 + 109.9 (see Figure 3.10B) and the mean + SEM for the ERBB4 KD group (n = 6) was 280.8 + 131.5 in Experiment 1 (see Figure 3.10C). In Experiment 2 (see Figure 3.11A), the mean + SEM for the ERBB4 NC group (n = 6) was 52.50 + 27.05 in (see Figure 3.11B) and the mean + SEM for the ERBB4 KD group (n = 6) was 32.50 + 15.33 (see Figure 3.11C). In experiments 1 and 2, the mean numbers of oligometastases per field are slightly reduced in the ERBB4 KD condition compared to the mean numbers of oligometastases in the ERBB4 NC condition. These differences were not found to be statistically significant in either experiment by student T-test, however. It is difficult to draw a larger conclusion about the influence of ERBB4 expression on formation of oligometastases from this data because of the means and spread of data between experiments. Thus, we compared ERBB4-positive and ERBB4-negative oligometastases within each experimental group to see if absence of ERBB4 expression in the KD condition significantly affected formation of oligometastases.

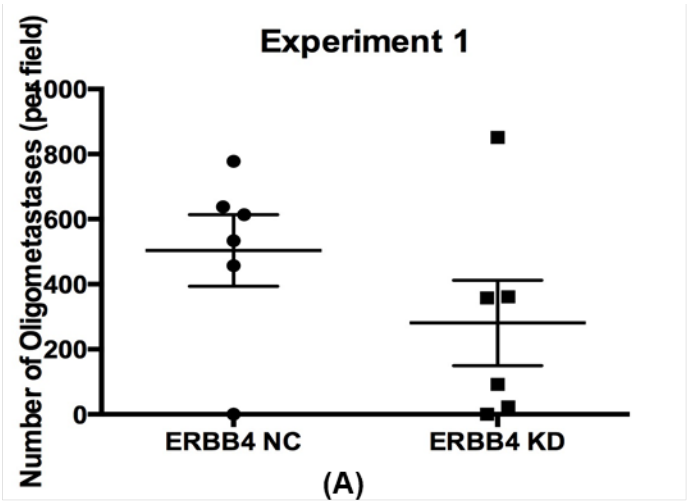


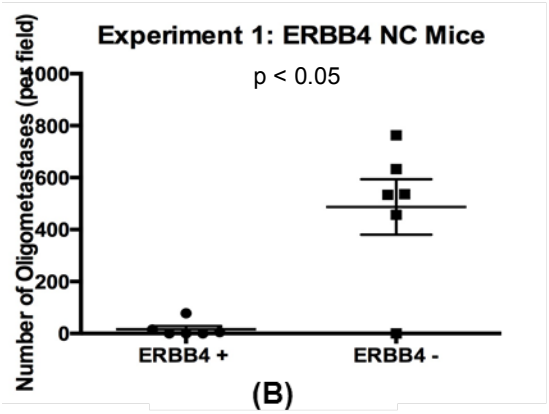


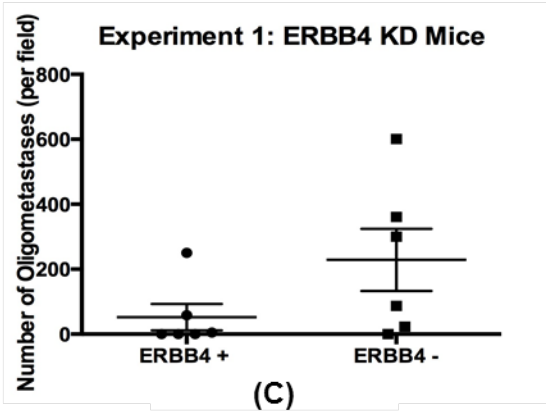


**Figure 3.10: The mean number of ERBB4-negative oligometastases per field is significantly greater than ERBB4-positive oligometastases in ERBB4 NC mice in Experiment 1 ($p < 0.05$) but mean oligometastases are not different between ERBB4 knockdown and scrambled control.** A. The mean number of oligometastases per field is lower in ERBB4 KD than ERBB NC but is not statistically significant. B. The mean number of ERBB4-negative oligometastases per field is significantly greater than ERBB4-positive oligometastases in ERBB4 NC mice in Experiment 1 ($p < 0.05$) C. The mean number of ERBB4-negative oligometastases per field is greater in ERBB4 KD mice in Experiment 1 but not significant. Lines + whiskers represent Mean + SEM of 6 mice.

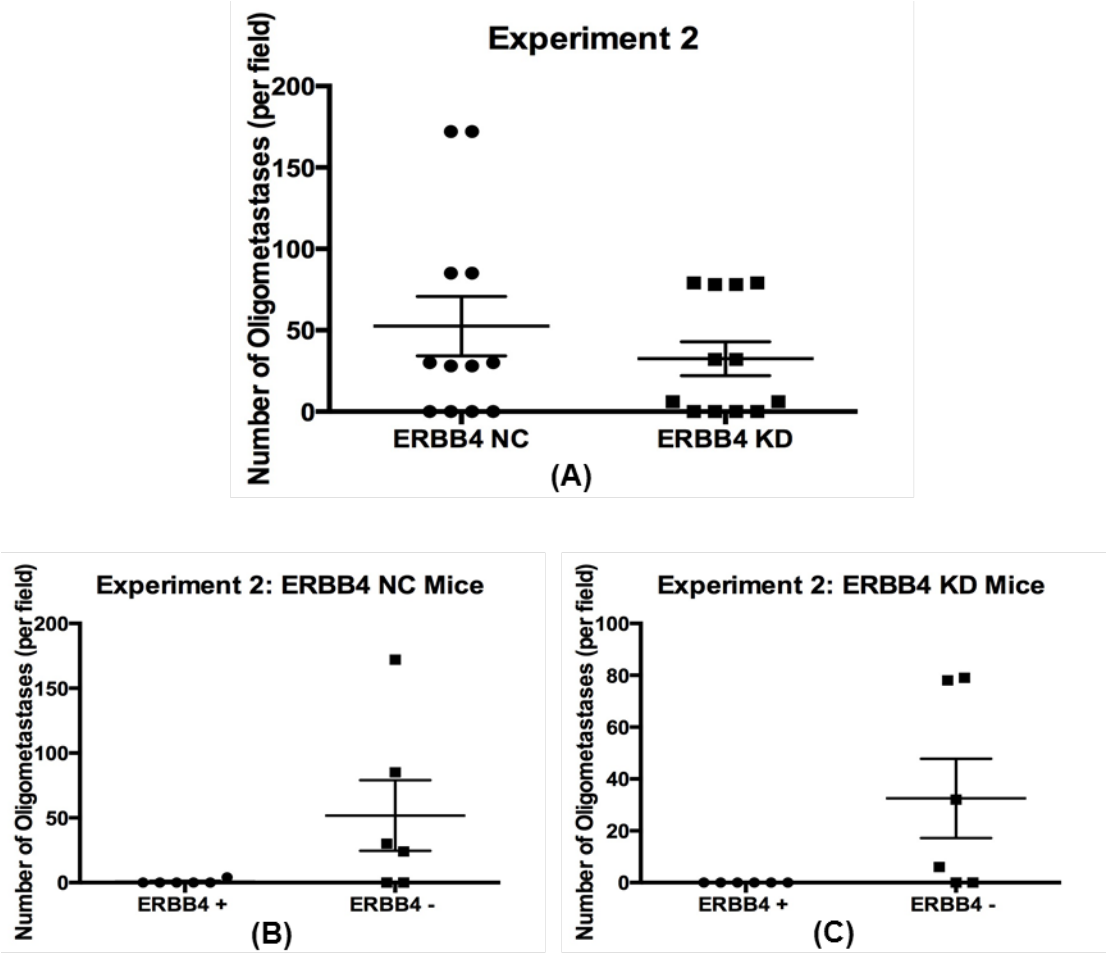


**Figure 3.11: There is no significant difference in mean number of oligometastases between the ERBB4 knockdown group and scrambled control group in Experiment 2.** A. There was a slight reduction in mean number of oligometastases with ERBB4 knockdown but it was not statistically significant. B. Oligometastases are primarily ERBB4-negative in scrambled control mice. C. Oligometastases are entirely ERBB4-negative in ERBB4 knockdown mice. Lines + whiskers represent Mean + SEM of 6 mice.

Our two separate experiments indicate that loss, or reduction of expression as seen in knockdown, of ERBB4 expression does not significantly impair the formation of oligometastases. The most compelling data to support this is seen in Experiment 1, where there are significantly greater mean ERBB4-negative oligometastases than ERBB4-positive oligometastases in the ERBB4 NC mice ($p < 0.05$) (see Figure 3.10B). There were experimental confounds that preclude larger conclusions from this data and that render our conclusions tentative. These will be elaborated upon further in the discussion.

### *3.2d ERBB4 knockdown results in a significant decrease in average ERBB4-negative metastases detected*

We hypothesized knockdown of ERBB4 would impair the formation of gross osteosarcoma metastases in the lungs of mice injected with CCH-OS-O cells with ERBB4 knockdown. To remain true to the data and honest to those who may find this thesis of any use in the future, it is best to say that the data presented in this section neither support nor refute this hypothesis. In spite of this preamble, there are interesting trends in this data that suggest that ERBB4 expression helps osteosarcoma cells form gross metastases in the lungs through the lack of ERBB4-expressing metastases in the ERBB4 NC condition.

We analyzed sections of lungs and tibias from mice that were given intra-tibial injections of the metastatic osteosarcoma line CCH-OS-O. There were ERBB4-positive and ERBB4-negative macrometastases and micrometastases in both ERBB4 KD and ERBB4 NC lungs. Additionally, the number and distribution of ERBB4-positive cells within gross CCH-OS-O lesions was highly variable. There were macrometastases of over 200 microns with areas of ERBB4 expression that were not more than 5-6 cells in size when examined under 40x magnification. In many slides, several micrometastases appeared to have more ERBB4-positive cells than the macrometastases in the same section

We needed a comparison to illustrate how lack of ERBB4 expression affects the formation of osteosarcoma metastases. Thus, we compared the total metastases in the ERBB4 NC condition to “ERBB4-negative” metastases in the ERBB4 KD mice. We defined an ERBB4-negative metastasis as a lesion with no detectable ERBB4-positive cells within our microscopic field. Any metastatic lesion with at least one ERBB4-positive cell was defined as “ERBB4-positive.” Although this will be expanded upon in the discussion, it is still important to acknowledge here that we did not adequately address variability of ERBB4 expression within and between lesions in this study. That was out of the scope of this thesis.

We first compared the mean macrometastases per field in the ERBB4 NC and ERBB4 KD groups in Experiments 1 and 2 (see Figure 3.12). There was a reduction of mean gross macrometastases detected per field in the ERBB4 KD condition from the ERBB4 NC condition in both experiments. The differences in mean gross metastases detected per field in ERBB4 NC vs. ERBB4 KD mice were statistically insignificant for both experiments.

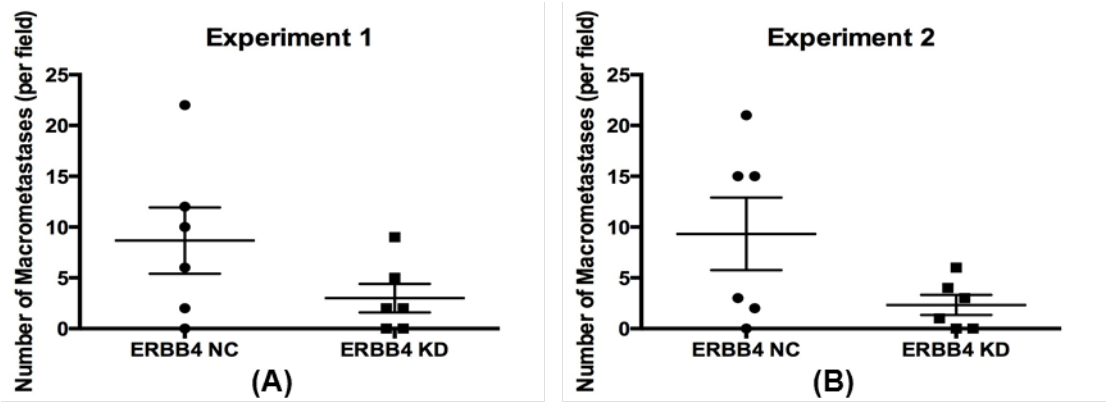


**Figure 3.12: The mean number of macrometastases per field is reduced in the ERBB4 KD group compared to the ERBB4 NC group in Experiments 1 and 2.** A. Results for Experiment 1. An average of 8.667 +3.252 macrometastases were detected per field in the ERBB4 NC condition. An average of 3.000 + 1.414 macrometastases were detected per field in the ERBB4 KD condition. This difference was not statistically significant. B. Results for Experiment 2. An average of 9.333 + 3.565 macrometastases were detected per field in the ERBB4 NC condition. An average of 2.333 + 0.989 macrometastases were detected per field in the ERBB4 KD condition. Lines + whiskers represent Mean + SEM of 6 mice.

Next, we compared mean ERBB4-positive metastases to mean ERBB4-negative macrometastases within the ERBB4 NC and ERBB4 KD groups in Experiment 1 and Experiment 2 (see Figure 3.13). There is a significant reduction in the formation of mean ERBB4-negative macrometastases per field to 0.0 in the ERBB4 NC group in Experiment 1 ($p < 0.05$) (see Figure 3.13A). An average of 8.333 + 3.190 ERBB4-positive macrometastases were detected per field in the ERBB4 NC group in Experiment 1 ($p < 0.05$) (see Figure 3.13A). An average of 2.333 + 0.989 ERBB4-negative macrometastases were detected per field in the ERBB4 NC group in Experiment 2, with an average of 9.333 + 3.565 ERBB4-positive

macrometastases detected per field within the same group (see Figure 3.13C). The difference was not statistically significant.

An unexpected finding in our experiment was the re-expression of ERBB4 in macrometastases and micrometastases in the ERBB4 KD groups from Experiments 1 and 2 (see Figures 3.12 and 3.14)**.** An average of 2.833 + 1.447 ERBB4-positive macrometastases were detected per field and an average of 0.333 + 0.211 ERBB4-negative macrometastases was detected per field in the ERBB4 KD group in Experiment 1 (see Figure 3.13B). Differences between these groups were statistically insignificant. For the ERBB4 KD group in Experiment 2, an average of 1.167 + 0.793 ERBB4-positive macrometastases was detected per field and an average of 1.167 + 0.601 ERBB4-negative macrometastases was detected per field (see Figure 3.13D). The average ERBB4-positive and ERBB4-negative macrometastases per field were not significantly different and were approximately equal in the ERBB4 KD group in Experiment 2.

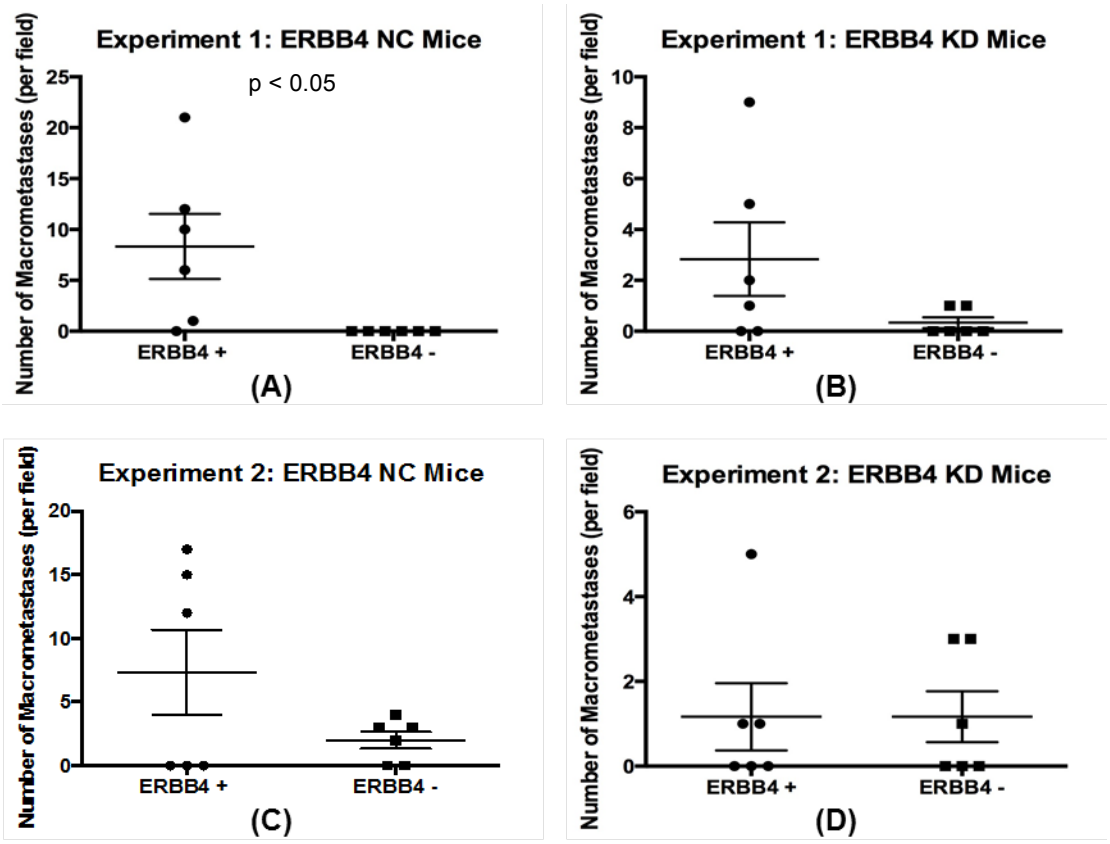


**Figure 3.13: Comparisons of average ERBB4-positive (ERBB4 +) macrometastases per field to average ERBB4-negative (ERBB4 -) macrometastases per field within experimental groups.** A. Average ERBB4-negative macrometastases per field were significantly reduced to 0.000 + 0.000 compared to mean ERBB4-positive macrometastases per field ($p < 0.05$). B. There was re-expression of ERBB4 in the macrometastases in the ERBB4 knockdown (KD) groups in Experiments 1 and 2. The mean ERBB4-negative macrometastases detected per field was decreased from the mean ERBB4-positive macrometastases per field in the ERBB4 knockdown group. C. Average ERBB4-negative macrometastases per field were lower compared to mean ERBB4-positive macrometastases per field. D. Re-expression of ERBB4 was seen in the ERBB4 knockdown (KD) group, with average 1.67 macrometastases detected per field in both the ERBB4 + and ERBB4 – groups. Lines + whiskers represent Mean + SEM of 6 mice.

### *3.2e ERBB4 Expression in Micrometastases*

We see in Experiment 1 that there is an average 5.333 + 2.060 micrometastases detected per field in ERBB4 KD group, which is significantly lower than the mean 17.000 + 4.546 micrometastases detected per field in ERBB4 NC group ($p < 0.05$) (see Figure 3.14A). Experiment 2 shows a similar trend of lower mean micrometastaes per field in the ERBB4 KD group, with an average 3.500 + 2.540 micrometastases per field in the ERBB4 KD group as

compared to an average 11.00 + 2.503 micrometastases per field in the ERBB4 NC group (see Figure 3.14B). The results were not statistically significant for Experiment 2.

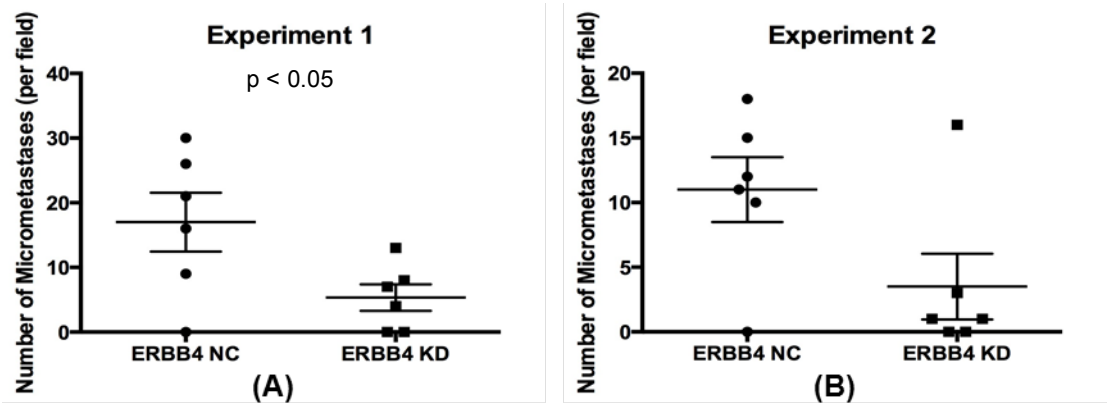


**Figure 3.14: The mean number of micrometastases per field is reduced in the ERBB4 KD group compared to the ERBB4 NC group in Experiments 1 and 2.** A. The average number of micrometastases per field is significantly lower in the ERBB4 KD condition than average number of micrometastases per field in the ERBB4 NC condition ($p < 0.05$). B. The mean number of micrometastases per field is lower in the ERBB4 KD than the mean number per field in the ERBB4 NC like in Experiment 2 but this was not significant. Lines + whiskers represent Mean + SEM of 6 mice.

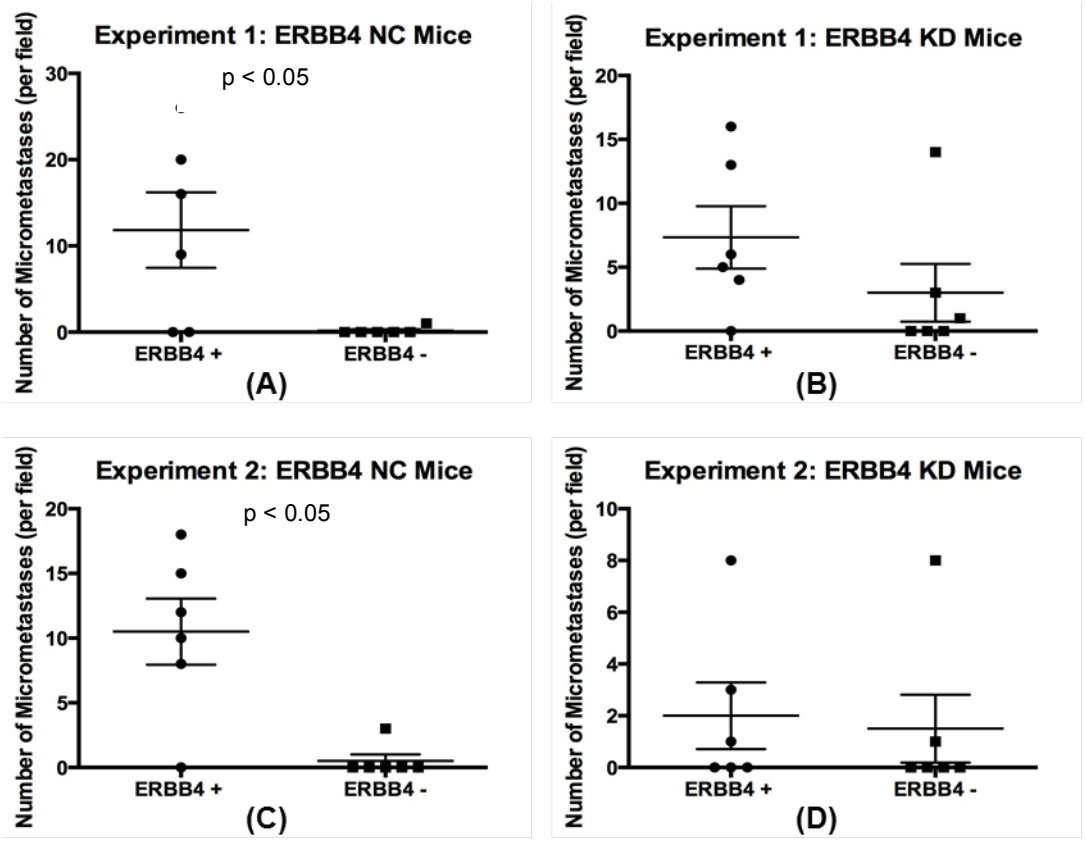


**Figure 3.15: Comparisons of average ERBB4-positive (ERBB4 +) micrometastases per field to average ERBB4-negative (ERBB4 -) micrometastases per field within experimental groups.** A. Average ERBB4 - micrometastases detected per field were significantly lower compared to mean ERBB4+ micrometastases detected per field ($p < 0.05$). B. There was re-expression of ERBB4 in micrometastases in ERBB4 KD mice in Experiment 1. C. Average ERBB4 - micrometastases detected per field were significantly lower compared to mean ERBB4+ micrometastases per field ($p < 0.05$). D. There was an average of 2.000 + 1.291 ERBB4+ micrometastases detected per field and an average of 1.500 + 1.310 ERBB4 – micrometastases detected per field in the ERBB4 KD condition. The difference was not significant. Lines + whiskers represent Mean + SEM of 6 mice.

In Experiments 1 and 2, the average ERBB4-negative mictrometastases detected per field were significantly lower the average ERBB4-positive micrometastases detected per field in both of the ERBB4 NC groups (see Figures 3.15A, 3.15C).There was an average of 11.83 + 4.370 ERBB4-positive micrometastases per field in the ERBB4 NC group in Experiment 1, compared with an average of 0.1667 + 0.1667 ERBB4 negative metastases per field detected ($p < 0.05$) (see Figure 3.15A). In the ERBB4 NC condition in Experiment 2, there was an average 10.50 + 2.553 ERBB4-positive micrometastases detected per field compared to an average 0.5000 + 0.5000 ERBB-negative micrometastases detected per field ($p < 0.05$) (see Figure 3.15C).

There was re-expression of ERBB4 in micrometastases in the ERBB4 KD groups of both experiments. There are higher average ERBB4-positive micrometastases detected per field than average ERBB4-negative micrometastases detected per field in the ERBB4 KD groups in Experiment 1 and Experiment 2 (see Figures 3.15B, 3.15D) . An average 7.333 + 2.445 ERBB4-positive micrometastases were detected per field in the ERBB4 KD condition in Experiment 1 with an average of 3.000 + 2.251 ERBB4-negative micrometastases detected per field (see Figure 3.15B). There was an average of 2.000 + 1.291 ERBB4 positive micrometastases detected per field and an average of 1.500 + 1.310 ERBB4 negative micrometastases detected per field in the ERBB4 KD condition in Experiment 2 (see Figure 3.15D). This increase in average ERBB4-positive micrometastases detected per field over average ERBB4-negative micrometastases detected per field in the ERBB4 KD groups is not surprising given the re-expression of ERBB4 in the ERBB4 KD mice but did not reach significance in Experiment 1 or Experiment 2.

### *3.2f Summary*

We see that there are fewer average ERBB4-positive macrometastases detected per field in the ERBB4 NC and KD conditions in Experiments 1 and 2. Overall, average macrometastasis formation was increased in the ERBB4 NC conditions for both experiments but these increases were not significant. There was a significant increase in average ERBB4-positive macrometastases detected per field in the ERBB4 NC group in Experiment 1 ($p < 0.05$) (see Figure 3.13A). There was a significant increase in average ERBB4-positive micrometastases detected in the ERBB4 NC group in Experiments 1 and 2 (see Figures 3.15A and Figure 3.15C). We see that formation of oligometastases is not impacted by lack of ERBB4 expression. The proportion of oligometastases expressing ERBB4 allows us to hypothesize that this data provides evidence for ERBB4 expression as not critical to the establishment of

oligometastases in the lungs. Due to the variability in ERBB4 expression in CCH-OS-O cells, it is difficult with this data to state definitively if ERBB4 re-expresses itself when seeded cells grow to detectable lesions or if some CCH-OS-O cells escaped knockdown and re-expressed ERBB4 in the metastatic lesions. Our knockdown efficiency was at 98%, as detected by Western blot. We also saw variability in ERBB4 expression in Western blots of CCH-OS-O monolayer cultures and in *in vivo* experiments that attempted to replicate this data. We could not consistently detect ERBB4 expression in CCH-OS-O cells by Western Blot. Due to lack of consistent ERBB4 expression patterns in CCH-OS-O, it is difficult to draw larger conclusions from this data. Trends from this data indicate that ERBB4 expression may aid metastatic progression in osteosarcoma, or growth of seeded cells into detectable metastases.

Comparing total metastases to "ERBB4-negative" metastases in CCH-OS-O was problematic in a cell line like CCH-OS-O with such variable expression, in hindsight. This definition sufficed for assessing ERBB4 expression in CCH-OS-O oligometastases because they were 1-5 cells in size and lacked significant 3-D structure. For micrometastases or macrometastases formed from CCH-OS-O, defining a lesion as "ERBB4-negative" meant that we may have missed sections containing at least one ERBB4-positive cell in lesions with more extensive 3-D structure.

# Chapter 4: Discussion

### 4.1 Cleavable Isoforms of ERBB4 Increase from Monolayer Culture to Tumor Spheroids

We wanted to find a mechanism for how ERBB4 promoted enhanced survival in tumor spheroids. qRT-PCR was performed on monolayer, high density and sphere cultures of four metastatic osteosarcoma cell lines that up-regulated ERBB4 protein expression in tumor spheres, multicellular aggregates of cells with tighter adhesion and areas of hypoxia and necrosis. Based on previous studies of ERBB4 expression in metastatic osteosarcoma cells that showed primarily nuclear ERBB4 expression, the hypothesis was there would be an increase in the proportion of the juxtamembrane cleavable isoforms of ERBB4 in anchorage-independent cultures from monolayer cultures of osteosarcoma [52]. This would provide a rationale for experiments to see if ERBB4 cleavage and downstream signaling of the resulting p80 fragment promoted enhanced cell survival and malignancy in osteosarcoma.

What did we learn from these experiments? There was a significant increase, either through proportion or up-regulation, of at least one cleavable isoform from monolayer to sphere culture in all of the cell lines. There was a significant increase in the proportion of cleavable isoforms expressed in tumor spheroids in CCH-OS-O ($p < 0.05$). The significant increase in Jm-a in CCH-OS-D, the predominant isoform expressed in CCH-OS-D, and Jm-a and Jm-d in Saos2 appears to be up-regulation due to the increase in both isoforms exceeding the absolute copy numbers of Jm-a and Jm-d isoforms in monolayer cultures ($p < 0.05$). CCH-OS-K up-regulated Jm-d expression significantly from expression levels in monolayer cultures that did not pass the threshold of detection by PCR ($p < 0.05$).

CCH-OS-D was selected for this experiment because it displayed prominent up-regulation of ERBB4 protein from monolayer to sphere cultures by Western blot. Our results predictably aligned with the earlier protein results, showing up-regulation of total ERBB4 mRNA from monolayer to sphere culture in CCH-OS-D. The up-regulation of ERBB4 mRNA

was driven primarily through an increase in transcription of the Jm-a isoform in CCH-OS-D, which supports our hypothesis.

Saos2 was of particular interest because of earlier findings that showed ERBB4 detected primarily as its MW 80,000 fragment in Western blots and immunohistochemistry performed on the cell line [75]. Total ERBB4 (MW 180,000) was up-regulated from monolayer to sphere cultures of Saos2 but the MW 80,000 fragment was not consistently detectable in monolayer or sphere cultures of our experiment. Seeing a loss of signal across cell lines that had previously shown p80 signal with this antibody and comparing the sequences of the antibodies provided by the manufacturer led us to conclude that this was due to a manufacturing-introduced change in the sequence of the antibody used for our Western blots. There was a significant increase in Jm-a and Jm-d isoform mRNA from monolayer to sphere cultures that resembled up-regulation more than a shift in proportion when compared to the absolute mRNA levels of Jm-b and Jm-c in monolayer culture.

A future experiment that follows from the findings above is a Western blot of the cell lines from our panel with an ERBB4-ICD selective antibody to detect the p80 antigen to uncover potential mechanisms for ERBB4 signaling in spheres. The p80 fragment has been causally linked to the difference in function between the Jm-a and Jm-b isoforms [78]. Designing an siRNA to specifically target the Jm-d antibody would also be interesting, as this may show if the Jm-d isoform is functionally meaningful through proteolytic cleavage in cell lines that up-regulate its expression in sphere cultures. Although Jm-d contains the splice site for proteolytic cleavage, it is currently debated if Jm-d is cleaved. This would be very helpful to further elucidating mechanisms of ERBB4 functioning.

We cannot state from these experiments alone if it is total ERBB4 protein expression or shift in isoform proportion that enhances survival in osteosarcoma spheres from the data

presented here. Transcription of Jm-a is increased in sphere cultures of Ewing sarcoma through E-cadherin mediated ERBB4 activation of the PI3-Akt pathway [77]. Treating ERBB4-expressing Ewing sarcoma cells with siRNA's targeted against various sequences of ERBB4 before plating them in anchorage-independent conditions yielded fewer spheres that were smaller in number [77]. We should have performed a similar experiment to see if reducing ERBB4 protein levels impacted sphere formation in the cell lines on our panel. qRT-PCR for total ERBB4 transcription levels should also have been included for all of the culture conditions in each cell line. It is still apparent from examining absolute mRNA copy numbers between isoforms in CCH-OS-D and CCH-OS-K that there is a total up-regulation of ERBB4 mRNA expression from monolayer to sphere cultures.

Measuring total ERBB4 mRNA levels in monolayer and sphere cultures of CCH-OS-O could begin to show if the changes in proportion are meaningful between culture conditions. This could be followed by monolayer and sphere cultures of CCH-OS-O cells with siRNA targeting of Jm-a isoform and siRNA targeting of ERBB4 respectively to compare differences in sphere formation. The experiments would provide proof-of-principle for the findings in this thesis.

CCH-OS-O had the lowest absolute copy numbers across isoforms and culture conditions of the cell lines on the panel, with numbers that were just past the threshold of detection for PCR. The quantity of Jm-a transcript increases (approximately 600 mRNA copy number/$10^6$ GAPDH) in near-direct proportion to the sum of absolute mRNA copy numbers of Jm-b, Jm-c and Jm-d (approximately 430 mRNA copy number/$10^6$ GAPDH) from monolayer to sphere culture. Differences in total transcript number between monolayer and sphere cultures could not be assessed for significance because total ERBB4 transcript levels in monolayer and

sphere cultures were not obtained in this experiment. The increase in Jm-a and decreases in Jm-b, Jm-c and Jm-d were all significant from monolayer to sphere in CCH-OS-O ($p < 0.05$).

The data in CCH-OS-O would have strengthened our hypothesis if CCH-OS-O had not displayed variable expression between different passages. In our experiment, CCH-OS-O monolayer cultures showed variable ERBB4 protein expression by Western blot between different passages. We selected CCH-OS-O because of ERBB4 protein up-regulation from monolayer to sphere cultures detected by previous Western blots in our laboratory. We could not consistently detect ERBB4 protein in CCH-OS-O monolayer cultures by Western blot using the same protocol and reagents as the previous experiments, however. CCH-OS-O expression in monolayer and sphere cultures just passed the threshold of detection by PCR in our experiments.

The variability of ERBB4 expression levels across cell lines is not unexpected. Tumor heterogeneity always poses a challenge to characterizing gene expression within a tumor type, especially one with high genomic variability and instability like osteosarcoma. It is hard to extrapolate generalizable conclusions from a model when the gene expression is inconsistent, however. It may be that ERBB4 expression is up-regulated to a threshold of detection in spheres but variably expressed in CCH-OS-O monolayer cells. CCH-OS-K spheres show significant up-regulation of Jm-b, Jm-c and Jm-d isoforms from monolayer expression levels that are so low as to not be quantifiable by PCR. CCH-OS-O is derived from a primary tumor, as are CCH-OS-D and Saos2. CCH-OS-D and Saos2 showed significant increases in expression of Jm-a and Jm-d isoforms in sphere culture. CCH-OS-O showed a significant increase in proportion of Jm-a isoform with proportionate decrease of Jm-b, Jm-c and Jm-d to Jm-a. The data in CCH-OS-O does not seem unreasonable when compared against the other data but further studies need to be conducted to understand the significance of a shift in proportion of cleavable isoforms in osteosarcoma spheres.

qRT-PCR could be performed to measure absolute ERBB4 mRNA copy number in monolayer and sphere cultures of the cell lines in our panel, as stated earlier. This data would be useful for placing the shifts in isoform proportion in context. Otherwise, increased proportion of cleavable isoform expression in sphere culture without an accompanying significant increase in absolute ERBB4 mRNA expression suggests that increased cleavable isoform expression is critical to sphere formation in osteosarcoma. Finding significant increases in proportion of cleavable isoforms expressed and total ERBB4 expression would strengthen that conclusion.

CCH-OS-K was derived from a malignant pleural effusion [62]. It was included on this panel because of up-regulation of total ERBB4 protein from monolayer to sphere cultures of the cell lines, the inclusion criteria for the cell lines on this panel. The other cell lines on the panel were derived from primary tumors that metastasized to the lungs. The PCR data for CCH-OS-K reveals that ERBB4 signaling could be altered greatly in osteosarcoma cells that survived without attachment to extracellular matrix *in vivo* compared to primary tumors.

There was significant up-regulation of the Jm-b, Jm-c and Jm-d isoforms in CCH-OS-K spheres. Although we lack data on absolute ERBB4 mRNA copy numbers in CCH-OS-K, we can still see that the absolute copy number of Jm-b in CCH-OS-K spheres was the highest copy number measured of any isoform across culture conditions and cell lines. Up-regulation of Jm-b was approximately 50-fold higher than that of Jm-c or Jm-d. In addition, the Jm-b copy number in CCH-OS-K spheres exceeds that of the approximate copy numbers of the other isoforms combined in CCH-OS-D, Saos2 and CCH-OS-K.

While it is insufficient to disprove our hypothesis, the data in CCH-OS-K requires us to consider that our hypothesis may be incorrect or more likely, needs to be refined. qRT-PCR studies for juxtamembrane isoform expression in monolayer and sphere cultures of an expanded panel of cell lines derived from malignant pleural effusions would be the most important next

step. If we did not see increases in proportion of cleavable isoforms across cell lines, it would force us to re-think our original hypothesis. There was significant up-regulation of the Jm-d cleavable isoform in CCH-OS-K in spheres but the proportion was smaller than that of the Jm-b and Jm-c isoforms expressed. This could mean that the proportions of ERBB4 isoforms shift in osteosarcoma cells depending on environmental demands *in vivo.* We do not know the mechanism by which CCH-OS-K cells reached the lung pleura, as malignant pleural effusions can result from metastasis or from a host of other mechanisms [79]. The cells were alive without attachment to matrix *in vivo*, which allows us to reasonably conclude that the programs enabling cellular survival in CCH-OS-K *in vivo* were altered from those enabling survival in the other cell lines that were derived from conditions of cell-cell and cell-matrix contact. Thus, it could be that the increase in cleavable isoform proportion in CCH-OS-D and CCH-OS-O and the up-regulation in Saos2 were early responses to loss of matrix attachment, or a response to a different stimulus entirely, from the up-regulation of Jm-b seen in CCH-OS-K.

It is possible that this experiment may have set groundwork for a novel mechanism by which Jm-b mediates anoikis resistance or more conservatively, response to some stress of the invasion-metastasis cascade in osteosarcoma. Jm-a is considered the pro-survival isoform, while Jm-b is shown to promote cell death in the face of stress [78]. The up-regulation of Jm-b in CCH-OS-K is unusual in the context of ERBB4 signaling in anchorage-independent survival of cells. Jm-a overexpression enhances anchorage-independent growth in fibroblasts while this effect was not observed with Jm-b overexpression [48]. Jm-a was also found to promote malignant behavior and survival in epithelial carcinomas, ependymomas and breast cancer while fibroblasts overexpressing Jm-b responded with apoptosis-like mechanisms to stresses like serum starvation [48].

Mutational analysis of ERBB4 on our cell lines may have shown if the expression difference in CCH-OS-K were due to mutation of the ERBB4 receptor expressed in CCH-OS-K. Studies of Jm-a signaling in pancreatic cancer spheroids found that wild-type ERBB4 enhanced NRG1-β stimulation of anchorage-independent growth while mutations in ERBB4 that prevented NRG1-β tyrosine phosphorylation did not enhance the effect of NRG1-β on anchorage independent growth [78]. Studies in breast cancer cells found that only Jm-a Cyt-2 was capable of promoting survival in a ligand-independent manner, with phosphorylation and generation of a signaling p80 fragment [78]. A mutated Jm-a isoform in CCH-OS-K could have resulted in up-regulation of the other isoforms to mediate anchorage-independent survival, especially Jm-d.

The isoform expression in the high density condition in this experiment is difficult to interpret because it did not serve its intended function. This condition was included to better understand the import of cell-cell contact on ERBB4 transcription, as cell-cell contact resulted in ERBB4 up-regulation in neuroblastoma and ERBB4 activation in Ewing tumor spheroids [52, 76]. We hypothesized that the high density culture condition would represent an intermediate in complexity and demands on cellular survival between monolayer and sphere cultures that would provide a clearer measure of the impact of cell-cell contact on ERBB4 expression [52]. As such, we predicted that we would see a significant increase in cleavable isoform proportion from monolayer to high density and a subsequent significant increase from high density to sphere culture.

We designed the experiment under the assumption that mechanisms of cell-cell contact were enhanced, but not altered, in tumor spheroids from adherent culture. First, tumor spheroids in our experiment were grown in anchorage-independent conditions while cells in the high density cultures had attached to extracellular matrix. We were ultimately comparing cell-cell

interactions in anoikis-resistant cells with cells influenced by cell-matrix interactions. Other phenomena associated with tumor spheroids that would introduce similar are hypoxic centers, areas of necrosis and alterations in gene expression in 3-D culture from 2-D culture [81]. There was no increase of expression of any isoform from monolayer to sphere culture in CCH-OS-K. There is an increase in expression of ERBB4 isoforms from monolayer cultures to high density cultures in CCH-OS-D and Saos2. The copy numbers of the Jm-b, Jm-c and Jm-d isoforms in CCH-OS-D across culture conditions relative to those of Jm-a demonstrate that the Jm-a is the predominant isoform expressed in in CCH-OS-D. The Jm-a isoform shows an increase in expression from monolayer to high density in CCH-OS-D but the increase is not significant. The increase in Jm-a copy number is significant from monolayer to sphere cultures ($p < 0.05$). High density cultures in Saos2 show an up-regulation of all of the isoforms from monolayer cultures but an increase in proportion to predominantly cleavable Jm-a and Jm-d isoforms in tumor spheroids. Expression of all isoforms decreased in high density from monolayer cultures of CCH-OS-O in spite of down-regulation of the other isoforms in proportion to the predominant expression of Jm-a from monolayer to sphere cultures.

The inconsistent results from the high density condition preclude any interpretation of the effect of enhanced culture confluence on ERBB4 signaling in metastatic osteosarcoma. The tumor spheres in our experiment were viable in anchorage-independent conditions, a hallmark of metastatic cells. Integrins have been implicated as crucial to anoikis resistance and the overall metastatic phenotype in osteosarcoma [82, 83]. Integrins are a class of receptors that mediates interactions between cells and the extracellular matrix and regulates diverse functions such as adhesion, proliferation, migration and angiogenesis [82]. Integrins are composed of α-subunits and β-subunits that link non-covalently to form integrins heterodimers, of which at least 25 heterodimers exist [82]. Treating Saos2 cells with an anti-α-4 integrin antibody increased

anoikis in anchorage-independent conditions [83]. Knockdown of the β-4 integrin reduced anchorage-independent survival and inhibited the formation of pulmonary osteosarcoma metastases in a mouse xenograft model [82]. Loss of β-4 integrin expression decreased anchorage-independent survival in osteosarcoma cells without affecting proliferation or cell morphology [82]. Additionally, β-4 integrin interacts with EGFR, ERBB2 and other RTK's to enhance oncogenic signaling [82]. Studying integrin-ERBB4 interactions in osteosarcoma holds promise for understanding the influence of cell-cell contact on ERBB4 expression.

The experiments outlined in this section showed an increase in juxtamembrane cleavable isoform mRNA from monolayer to sphere cultures of osteosarcoma. This argues for a role of the cleavable isoforms of ERBB4 in mediating responses to stress encountered in the invasion-metastasis cascade. We also had an interesting finding with CCH-OS-K up-regulating the Jm-b isoform in anchorage-independent conditions although Jm-a is the isoform that was predominantly up-regulated in studies of anchorage-resistance in other cancers. CCH-OS-K is derived from a malignant pleural effusion, or cells that have gained resistance to anoikis. Much work still remains to be done. The studies in this section introduce some useful findings to guide the study of ERBB4 signaling in osteosarcoma.

**4.2 ERBB4 expression is increased in osteosarcoma metastases**

Immunohistochemical staining of osteosarcoma metastases in the lungs of mice injected with CCH-OS-O knockdown (KD) cells and ERBB4 normal control (NC) cells was performed to see if ERBB4 was necessary for establishment of osteosarcoma metastases. Detectable metastases are the end product of the "invasion-metastasis cascade," a series of programmed, step-wise events undergone by metastatic cells to establish lesions at distant sites [71]. The events were initially described for carcinomas but experimental data shows that osteosarcoma metastases follow this series of events as well [70]. Cells from the primary tumor (1) *invade*

through the local extracellular matrix, (2) *intravasate* into blood vessels (3) *survive* circulation through the vasculature, or hematogenous spread (4) *arrest,* or stop at a distant site from the primary tumor, (5) *extravasate* into the tissue of the distant site (6) form *micrometastases* and (7) resume cellular programs that enable their growth into clinically detectable metastases, known as "metastatic progression [71]."

The experiments were analyzed separately because the scatter of the experiments showed that they could not be analyzed as replicates. The immunohistochemistry of the ERBB4 NC condition in Experiment 1 shows reduced formation of ERBB4-negative foci than ERBB4-positive foci ($p < 0.05$), suggesting that metastatic progression is significantly impaired in osteosarcoma *in the absence* of ERBB4 expression. There were significantly fewer ERBB4-negative micrometastases detected than ERBB4-positive micrometastases in the ERBB4 KD and NC groups of Experiment 1 ($p < 0.05$), which fits with the findings in macrometastases. Our knockdown efficiency was 98% as detected by Western blot prior to injection. Re-expression of ERBB4 was observed in pulmonary Ewing sarcoma metastases after ERBB4 KD and osteosarcoma pulmonary metastases re-expressed β-4 integrin with knockdown so this is not uncommon [51, 82]. The difference in numbers of oligometastases, or metastastic lesions of 1-5 cells, in the ERBB4 KD and NC lungs was not statistically significant. This could indicate that ERBB4 is not necessary to osteosarcoma cells surviving the metastatic cascade.

Analyses were performed on the mouse lungs to see if there was nuclear ERBB4-positive staining in lung metastases. We did not see any nuclear localization of ERBB4 in any tmetastases. There was only cytoplasmic staining of ERBB4 in all of the cells. This is not surprising given that CCH-OS-O expression varies by cell passage as discussed in the previous section.

The experiment could have been used to answer a fundamental question: is ERBB4 is necessary for osteosarcoma metastasis? The flaws with the model, coupled with the analyses undertaken to interpret data from a flawed model, render these inadequate results to answer that question. As presented here, the data suggests that ERBB4 is important to metastatic progression of osteosarcoma, the final step of the invasion-metastasis cascade. The current experiment could be repeated with mouse models that reliably form ERBB4-expressing pulmonary foci to answer this question.

We used CCH-OS-O, a metastatic osteosarcoma line, for our *in vivo* model. It is established that gene expression changes in cancer cell lines with passaging. We did not see consistent expression of ERBB4 protein in CCH-OS-O monolayer cultures by Western blot. Array genomic hybridization and microarray analysis of gene expression in osteosarcoma cell lines shows substantial chromosomal instability and gene expression alteration, especially in metastatic cell lines [84]. Because chromosomal instability is so high in osteosarcoma cell lines, it is suggested that several viable stocks of biopsy be frozen for *in vivo* osteosarcoma studies [84]. Flow cytometry for cell surface proteins like ERBB4 could also be used to ensure that ERBB4 expression levels were consistent

It logically follows from using a cell line with variable expression of ERBB4 that the expression patterns of ERBB4 were variable within lung metastases. Strength of ERBB4 staining varied within the lesions, as independently verified within our laboratory and by faculty in the Department of Pathology at MD Anderson. Strength of ERBB4 staining did not seem to be correlated with size. Several macrometastases showed just small portions of the lesion with ERBB4-positivity while some micrometastases were entirely positive for ERBB4. From gross inspection, it seemed as if some micrometastases possessed more ERBB4-positive cells than did macrometastases.

We counted all metastases with at least one ERBB4-positive viable cell as ERBB4-positive for the purposes of the experiment, as the variability was interpreted as ERBB4 expression itself being crucial to metastasis regardless of quantity or distribution. This would have been a sufficiently sensitive measure had CCH-OS-O consistently expressed ERBB4. Since metastases are three-dimensional and we were viewing sections, lesions were likely missed that were ERBB4-positive by our criterion.

The overall picture provided by the data is still worth considering. It appears that ERBB4 becomes more important during metastatic progression of osteosarcoma, which aligns with the findings in the previous study that ERBB4. Findings in NSCLC show that ERBB4 immunostaining was strong in tumors that metastasized to lymph nodes and weak in non-metastatic tumors [85]. An interesting direction would be to see if ERBB4 is critical to tumor-microenvironment interactions between the metastases and lung.

### 4.3 Future Directions

This thesis ultimately provided preliminary data that indicated some future directions for research on ERBB4 in osteosarcoma and solid tumors. The limitations in the design of both presented studies offer little in the way of conclusive directions. As such, several future experiments were outlined in sections 4.1 and 4.2.

Here are the broader directions to be taken in ERBB4 signaling in osteosarcoma. First, studies must be done to understand the expression and behavior of the p80 fragment in osteosarcoma cell lines to understand the increase in cleavable isoform expression in spheres. The function of the cleaved p80 fragment of ERBB4 in osteosarcoma cells is of interest, as it serves both oncogenic and tumor-suppressive roles in various cancers. Saos2 was the cell line used in our experiment with expression of primarily the MW 80,000 fragment. [76]. We did not consistently see the p80 fragment in Western blots of Saos2 in our laboratory but recent studies

of Saos2 show that gene expression is highly unstable with passaging of the cell line [84]. We could test if cleavage of ERBB4 is important to osteosarcoma is to add a TACE or gamma-secretase inhibitor to monolayer and sphere cultures of osteosarcoma. If survival in spheres is reduced after administration of the inhibitor, it may be worthwhile to test a TACE-inhibitor or gamma-secretase inhibitor that would halt cleavage of ERBB4 in patients with osteosarcoma. Phosphorylation of ERBB4 in the cell lines of our experiments should also be assessed with Western blot.

We did not study the influence of ERBB4 cytoplasmic isoform expression on ERBB4-enhanced multicellular survival in osteosarcoma. Both cytoplasmic isoforms are expressed in tissues that express ERBB4 but proportions of the Cyt-1 and Cyt-2 isoforms vary between tissues. The Cyt-1 isoform also contains a binding region for PI3K/Akt, which displays aberrant tumorigenic signaling in several cancers [7]. This line of investigation must be addressed with further studies for completeness in the study of ERBB4 receptor signaling.

ERBB4 is mutated in several cancers, which alters its signaling and responses to ligands [51]. Given that ERBB4 is expressed more abundantly in osteosarcoma metastases than primary tumors, sequencing ERBB4 in primary tumors and lung metastases may provide insight into differences in the receptors that begin to explain why and how it is up-regulated in osteosarcoma metastases. Developing isoform-specific siRNA to target ERBB4 in osteosarcoma metastases may also be a way to reduce metastatic burden in patients with ERBB4-positive osteosarcoma. The siRNA could be delivered in liposomes that are specific for tumor cells.

Previous unpublished data from patient-derived material shows that ERBB4 expression is stronger in osteosarcoma lung metastases than primary tumors (Hughes Laboratory). Antibodies that are specifically designed to target the Jm-a and Jm-b isoforms have been developed and used in breast cancer to halt ERBB4 phosphorylation and cleavage [50]. It may

be of benefit to administer antibodies that specifically target the most abundant isoforms of ERBB4 expressed within the primary tumor in the hopes of halting metastasis. A challenge to translating this finding to the clinic is the *in vivo* re-expression of ERBB4 in osteosarcoma in lung metastases after its gene expression is silenced in primary tumors, as demonstrated in the immunohistochemical findings presented in this thesis. A proposed solution would be to sequence the ERBB4 receptors expressed in the primary tumor and lung metastases and to deliver liposomal siRNA that specifically targets the ERBB4 variants expressed in the primary tumor and lung metastases. Finding the mechanism of ERBB4 function in osteosarcoma may be of great clinical value in metastatic osteosarcoma or the prevention of osteosarcoma metastasis.

Finally, ERBB4 may be an example of how shifting our current paradigm of treatment and identification of therapeutic markers and endpoints may yield benefit. New insights into solid tumor metastasis show that targeting metastatic progression of solid tumors could be of great therapeutic benefit, especially to osteosarcoma patients who are assumed to have metastatic disease progression even after metastases are seen on imaging [70]. ERBB4 could be a direct target for preventing progression of lesions and maintaining stable disease in patients who already possess clinically detectable metastases. ERBB4 is an intriguing and promising target in osteosarcoma metastasis.

## Bibliography


1. Luetke, A., et al., *Osteosarcoma treatment – Where do we stand? A state of the art review.* Cancer Treatment Reviews, 2014. **40**(4): p. 523-532.
2. Zhu, L., M.M. McManus, and D.P. Hughes, *Understanding the Biology of Bone Sarcoma from Early Initiating Events through Late Events in Metastasis and Disease Progression.* Front Oncol, 2013. **3**: p. 230.
3. Broadhead, M.L., et al., *The molecular pathogenesis of osteosarcoma: a review.* Sarcoma, 2011. 2011:959248. doi: 10.1155/2011/959248
4. Tarkkanen, M., et al., *Gains and losses of DNA sequences in osteosarcomas by comparative genomic hybridization.* Cancer Res, 1995. **55**(6): p. 1334-8.
5. Overholtzer, M., et al., *The presence of p53 mutations in human osteosarcomas correlates with high levels of genomic instability.* Proc Natl Acad Sci U S A, 2003. **100**(20): p. 11547-52.
6.. Ullrich, A. and J. Schlessinger, *Signal transduction by receptors with tyrosine kinase activity.* Cell, 1990. **61**(2): p. 203-212.
7. Yarden, Y. and M.X. Sliwkowski, *Untangling the ErbB signalling network.* Nat Rev Mol Cell Biol, 2001. **2**(2): p. 127-37.
8. Valley, C.C., K.A. Lidke, and D.S. Lidke. *The spatiotemporal organization of ErbB receptors: insights from microscopy.* Cold Spring Harb Perspect Biol, 2014. **6**(2).
9. Fry, W.H., et al., *Mechanisms of ErbB receptor negative regulation and relevance in cancer.* Exp Cell Res, 2009. **315**(4): p. 697-706.
10. Marmor, M.D., K.B. Skaria, and Y. Yarden, *Signal transduction and oncogenesis by ErbB/HER receptors.* Int J Radiat Oncol Biol Phys, 2004. **58**(3): p. 903-13.
11. Kraus, M.H., *All ErbB Receptors Other Than the Epidermal Growth Factor Receptor Are Endocytosis Impaired.* Journal of Biological Chemistry, 1996. **271**(9): p. 5251-5257.

12. Britten, C.D. *Targeting ErbB receptor signaling: a pan-ErbB approach to cancer.* Mol Cancer Ther, 2004. **3**(10): p. 1335-42.

13. Schlessinger, J. and M.A. Lemmon, *Nuclear signaling by receptor tyrosine kinases: the first robin of spring.* Cell, 2006. **127**(1): p. 45-8.

14. Bublil, E.M. and Y. Yarden, *The EGF receptor family: spearheading a merger of signaling and therapeutics.* Curr Opin Cell Biol, 2007. **19**(2): p. 124-34.

15. Olayioye, M.A., et al., *The ErbB signaling network: receptor heterodimerization in development and cancer.* EMBO J, 2000. **19**(13): p. 3159-67.

16. Carriere, A., et al., *The RSK factors of activating the Ras/MAPK signaling cascade.* Front Biosci, 2008. **13**: p. 4258-75.

17. Hoque, M., et al., *Annexins - Scaffolds modulating PKC localization and signaling.* Cell Signal, 2014. **26**(6): p. 1213-1225.

18. Vecchi, M., J. Baulida, and G. Carpenter, *Selective cleavage of the heregulin receptor ErbB-4 by protein kinase C activation.* J Biol Chem, 1996. **271**(31): p. 18989-95.

19. Sundvall, M., et al., *Isoform-specific monoubiquitination, endocytosis, and degradation of alternatively spliced ErbB4 isoforms.* Proc Natl Acad Sci U S A, 2008. **105**(11): p. 4162-7.

20. Arteaga, Carlos L. and Jeffrey A. Engelman, *ERBB Receptors: From Oncogene Discovery to Basic Science to Mechanism-Based Cancer Therapeutics.* Cancer Cell, 2014. **25**(3): p. 282-303.

21. Muraoka-Cook, R.S., et al., *The intracellular domain of ErbB4 induces differentiation of mammary epithelial cells.* Mol Biol Cell, 2006. **17**(9): p. 4118-29.

22. Ma, L., et al., *Ligand-dependent recruitment of the ErbB4 signaling complex into neuronal lipid rafts.* J Neurosci, 2003. **23**(8): p. 3164-75.

23. Gilbertson, R., et al., *Novel ERBB4 juxtamembrane splice variants are frequently expressed in childhood medulloblastoma.* Genes Chromosomes Cancer, 2001. **31**(3): p. 288-94.

24. Zeng, N., et al., *Real-time quantitative polymerase chain reaction (qPCR) analysis with fluorescence resonance energy transfer (FRET) probes reveals differential expression of the four*

*ERBB4 juxtamembrane region variants between medulloblastoma and pilocytic astrocytoma.* Neuropathol Appl Neurobiol, 2009. **35**(4): p. 353-66.

25. Sundvall, M., et al., *Differential nuclear localization and kinase activity of alternative ErbB4 intracellular domains.* Oncogene, 2007. **26**(48): p. 6905-14.

26. Law, A.J., et al., *Disease-associated intronic variants in the ErbB4 gene are related to altered ErbB4 splice-variant expression in the brain in schizophrenia.* Hum Mol Genet, 2007. **16**(2): p. 129-41.

27. Komuro, A., et al., *WW domain-containing protein YAP associates with ErbB-4 and acts as a co-transcriptional activator for the carboxyl-terminal fragment of ErbB-4 that translocates to the nucleus.* J Biol Chem, 2003. **278**(35): p. 33334-41.

28. Naresh, A., et al., *The ERBB4/HER4 intracellular domain 4ICD is a BH3-only protein promoting apoptosis of breast cancer cells.* Cancer Res, 2006. **66**(12): p. 6412-20.

29. Aqeilan, R.I., et al., *Association of Wwox with ErbB4 in breast cancer.* Cancer Res, 2007. **67**(19): p. 9330-6.

30. Chuu, C.P., et al., *Systems-level analysis of ErbB4 signaling in breast cancer: a laboratory to clinical perspective.* Mol Cancer Res, 2008. **6**(6): p. 885-91.

31. Sudol, M. and T. Hunter, *NeW wrinkles for an old domain.* Cell, 2000. **103**(7): p. 1001-4.

32. Schuchardt, B.J., et al., *Molecular origin of the binding of WWOX tumor suppressor to ErbB4 receptor tyrosine kinase.* Biochemistry, 2013. **52**(51): p. 9223-36.

33. Nowakowska, M., et al., *The correlation analysis of WWOX expression and cancer related genes in neuroblastoma- a real time RT-PCR study.* Acta Biochim Pol, 2014. **61**(1): p. 91-7.

34. Pluciennik, E., et al., *Genetic alterations of WWOX in Wilms' tumor are involved in its carcinogenesis.* Oncol Rep, 2012. **28**(4): p. 1417-22.

35. Williams, C.C., et al., *The ERBB4/HER4 receptor tyrosine kinase regulates gene expression by functioning as a STAT5A nuclear chaperone.* J Cell Biol, 2004. **167**(3): p. 469-78.

36. Ota, I., et al., *Heparin-binding EGF-like growth factor enhances the activity of invasion and metastasis in thyroid cancer cells.* Oncol Rep, 2013. **30**(4): p. 1593-600.

37. Maatta, J.A., et al., *Proteolytic cleavage and phosphorylation of a tumor-associated ErbB4 isoform promote ligand-independent survival and cancer cell growth.* Mol Biol Cell, 2006. **17**(1): p. 67-79.

38. Starr, A., et al., *ErbB4 increases the proliferation potential of human lung cancer cells and its blockage can be used as a target for anti-cancer therapy.* Int J Cancer, 2006. **119**(2): p. 269-74.

39. Prickett, T.D., et al., *Analysis of the tyrosine kinome in melanoma reveals recurrent mutations in ERBB4.* Nat Genet, 2009. **41**(10): p. 1127-32.

40. Lau, C., et al., *ERBB4 mutation analysis: emerging molecular target for melanoma treatment.* Methods Mol Biol, 2014. **1102**: p. 461-80.

41. Rudloff, U. and Y. Samuels, *A growing family: adding mutated Erbb4 as a novel cancer target.* Cell Cycle, 2010. **9**(8): p. 1487-503.

42. Fujiwara, S., et al., *Association of ErbB1-4 expression in invasive breast cancer with clinicopathological characteristics and prognosis.* Breast Cancer, 2012.

43. Gallo, R.M., et al., *Multiple Functional Motifs Are Required for the Tumor Suppressor Activity of a Constitutively-Active ErbB4 Mutant.* J Cancer Res Ther Oncol, 2013. **1**(1): p. 10.

44. Veikkolainen, V., et al., *Function of ERBB4 is determined by alternative splicing.* Cell Cycle, 2011. **10**(16): p. 2647-57.

45. Paatero, I. and K. Elenius, *ErbB4 and its isoforms: patentable drug targets?* Recent Pat DNA Gene Seq, 2008. **2**(1): p. 27-33.

46. Hollmen, M., et al., *Proteolytic processing of ErbB4 in breast cancer.* PLoS One, 2012. **7**(6): p. e39413.

47. Vidal, G.A., et al., *Presenilin-dependent gamma-secretase processing regulates multiple ERBB4/HER4 activities.* J Biol Chem, 2005. **280**(20): p. 19777-83.

48. Sundvall, M., et al., *Cell death or survival promoted by alternative isoforms of ErbB4.* Mol Biol Cell, 2010. **21**(23): p. 4275-85.

49. Paatero, I., et al., *Interaction with ErbB4 promotes hypoxia-inducible factor-1alpha signaling.* J Biol Chem, 2012. **287**(13): p. 9659-71.

50. Hollmen, M., et al., *Suppression of breast cancer cell growth by a monoclonal antibody targeting cleavable ErbB4 isoforms.* Oncogene, 2009. **28**(10): p. 1309-19.

51. Mendoza-Naranjo, A., et al., *ERBB4 confers metastatic capacity in Ewing sarcoma.* EMBO Mol Med, 2013. **5**(7): p. 1019-34.

52. Hua, Y., et al., *Slow down to stay alive: HER4 protects against cellular stress and confers chemoresistance in neuroblastoma.* Cancer, 2012. **118**(20): p. 5140-54.

53. Kang, H.G., et al., *E-cadherin cell-cell adhesion in ewing tumor cells mediates suppression of anoikis through activation of the ErbB4 tyrosine kinase.* Cancer Res, 2007. **67**(7): p. 3094-105.

54. Hirschhaeuser, F., et al., *Multicellular tumor spheroids: an underestimated tool is catching up again.* J Biotechnol, 2010. **148**(1): p. 3-15.

55. Kim, Y.N., et al., *Anoikis resistance: an essential prerequisite for tumor metastasis.* Int J Cell Biol, 2012. **2012**: p. 368-379.

56. Klein, C.A., *Parallel progression of primary tumours and metastases.* Nat Rev Cancer, 2009. **9**(4): p. 302-12.

57. Nguyen, D.X., P.D. Bos, and J. Massague, *Metastasis: from dissemination to organ-specific colonization.* Nat Rev Cancer, 2009. **9**(4): p. 274-84.

58. Junttila, T.T., et al., *Cleavable ErbB4 isoform in estrogen receptor-regulated growth of breast cancer cells.* Cancer Res, 2005. **65**(4): p. 1384-93

59. Richards, K., et al., *Signaling of ERBB Receptor Tyrosine Kinases Promotes Neuroblastoma Growth* in vitro *and* in vivo. Cancer, 2010, **116**(13): p.3233-3243.

60. Fischer, A.H., et al., *Hematoxylin and eosin staining of tissue and cell sections.* CSH Protoc, 2008,: p. pdb prot4985.

61. Simpson, C.D., K. Anyiwe, and A.D. Schimmer, *Anoikis resistance and tumor metastasis.* Cancer Lett, 2008. **272**(2): p. 177-85.

62. Huang, G., et al., *miR-20a encoded by the miR-17-92 cluster increases the metastatic potential of osteosarcoma cells by regulating Fas expression.* Cancer Res, 2012. **72**(4): p. 908-16.

63. Schiavo, R., et al., *Establishment and characterization of a new Ewing's sarcoma cell line from a malignant pleural effusion.* Anticancer Res, 2007. **27**(5A): p. 3273-8.

64. Strauss, S.J., et al., *Understanding micrometastatic disease and Anoikis resistance in ewing family of tumors and osteosarcoma.* Oncologist, 2010. **15**(6): p. 627-35.

65. Tao, R. and I. Maruyama, *All EGF(ErbB) receptors have preformed homo- and heterodimeric structures in living cells.* J Cell Sci, 2010. **121** p. 3207-17.

66. Kraus, M., et al., *Isolation and characterization of ERBB3, a third member of the ERBB/epidermal growth factor receptor family: Evidence for overexpression in a subset of human mammary tumors.* Proc. Natl Acad. Sci., 1989, **85**, p. 9193-97.

67. Press, M.F., et al. *Expression of the Her-2/neu proto-oncogene in normal human adult and fetal tissues.* Oncogene, 1990, **5**(7): 953-62.

68. Graus-Porta, D., et al. *ErbB-2, the preferred heterodimerization partner of all ErbB receptors, is a mediator of lateral signaling.* The EMBO Journal, 1997, **16**(7): p. 1647-55.

69. Hakanson, M., et al. *Controlled Breast Cancer Microarrays for the Deconvolution of Cellular Multilayering and Density Effects upon* Drug *Resistance.* PLOS, 2012, DOI: 10.1371/journal.pone.0040141

70. Khanna, C., et al. *Towards a Drug Development Path that Targets Metastatic Progression in Osteosarcoma.* Clinical Cancer Research, 2014, **20**(4200): DOI: 10.1158/1078-0432.CCR-13-2574.

71. Valastyan, S. and R.A. Weinberg. *Tumor Metastasis: Molecular Insights and Evolving Paradigms.* Cell, 2011, **147**(2): p. 275-92.

72. Purevdorj, E., et al. *ErbB4 deletion leads to changes in lung function and structure similar to bronchopulmonary dysplasia.* American Journal of Physiology-Lung Cellular and Molecular Physiology, 2008, **294**(3): p. L516-L522.

73. Citri, A. and Y. Yarden. *EGF-ERBB signaling: towards the systems level.* Nature Reviews Molecular Cell Biology, 2006, **7,** p. 505-516.

74. Linggi, B. and G. Carpenter. *ErbB receptors: new insights on mechanisms.* Trends in Cell Biology, 2006, **16**(12), p. 649-656.

75. Hughes, D.P., et al. *Cell surface expression of epidermal growth factor receptor and Her-2 with nuclear expression of Her-4 in osteosarcoma.* Cancer Research, 2004, **64**(6): p 2047-2053.

76. Hughes, D.P., et al. *Essential erbB family phosphorylation in osteosarcoma as a target of CI-1033 inhibition.* Pediatric Blood and Cancer, 2006, **46**(5): p. 2047-2053.

77. Kang, H.G., et al. *E-cadherin cell-cell adhesion in ewing tumor cells mediates suppression of anoikis through activation of the ErbB4 tyrosine kinase.* Cancer Research, 2007, **67**(6): p. 3094-105.

78. Maatta, J.M., et al. *Proteolytic cleav*age *and phosphorylation of a tumor-associated ErbB4 isoform promote ligand-independent survival and cancer cell growth.* Molecular Biology of the Cell, 2006, **17**(1): p 67-79.

79. American Thoracic Society. *Management of Malignant Pleural Effusions.* American Journal of Respiratory and Critical Care Medicine, 2000, **162**(5): p. 1987-2001.

80. Mill, C.P., et al. *Ligand stimulation of ErbB4 and a constitutively-active ErbB4 mutant result in different biological responses in human pancreatic tumor cell lines.* Experimental Cell Research, 2011, **31**7(4): p. 392-404.

81. Hirschhaeuser, F., et al. *Multicellular tumor spheroids: an underestimated tool is catching up again.* Journal of Biotechnology, 2010, **148**(1): p. 3-15.

82. Wan, X., et al. *Beta4-integrin promote*s *osteosrcoma metastasis and interacts with ezrin.* Oncogene, 2009, **28**(38): p. 3401-3411.

83. Marco, R.A.W., et al. *α4 integrin increases anoikis of human osteosarcoma cells.* Journal of Cellular Biochemistry, 2003, **88**(5): p. 1038-1047.

84. Muff, R., et al. Genomic instability of osteosarcoma cell lines in culture: impact on the prediction of *metastasis relevant genes.* PLOS One, 2015 May 19, 10(5): doi: 10.1371/journal.pone.0125611.

85. Starr, A., et al. *ErbB4 increases the proliferation potential of human lung cancer cells and its blockage can be used as a target for anti-cancer therapy.* International Journal of Cancer, 2006, **19** (2), 269-274.

**Vita**

Nupur Lala was born in Syracuse, New York and moved throughout her childhood to North Carolina, Florida and Fayetteville, Arkansas. She graduated from Fayettteville High School in Fayetteville, Arkansas in 2003 and received a Bachelor of Science in Brain, Behavior and Cognitive Sciences from the University of Michigan in 2007. Her interest in studying language processing and memory took her to the Department of Brain and Cognitive Sciences at MIT shortly after graduation, where she worked as a technical assistant in the Cognitive and Affective Neuroscience Laboratory on studies relating to motor skills acquisition, visual scene memory and fluid intelligence from 2007 to 2010. She pursued a Masters' of Science in Biomedical Sciences at the University of Texas Health Science Center at Houston/MD Anderson Cancer Center, where she graduated with a Masters of Biomedical Sciences in 2015. She is currently a candidate for the Doctor of Medicine (M.D.) at the University of Arkansas for Medical Sciences.